Discontinuous Adoption Dynamics and Token Valuation in Blockchain Platforms

Pascal Stiefenhofer *

Posted Date: 23 March 2026

doi: 10.20944/preprints202603.1720.v1

Keywords: dynamic token valuation; discontinuous adoption dynamics; filippov differential inclusions; network effects; nonsmooth dynamical systems; sliding modes; speculative behavior; cryptocurrency volatility; stability analysis; behavioral finance; threshold switching; nonlinear feedback; platform economics

 doi:10.20944/preprints202603.1720.v1

Article

Discontinuous Adoption Dynamics and Token Valuation in Blockchain Platforms

Pascal Stiefenhofer

Newcastle University, United Kingdom; pascal.stiefenhofer@newcastle.ac.uk

Abstract

This paper studies platform environments in which participation incentives change discontinuously when valuation crosses salient thresholds. Empirical research on digital and tokenized platforms documents valuation plateaus, abrupt participation shifts, and weak short-run links between price stability and usage dynamics, patterns that are difficult to reconcile with smooth adjustment models. We capture these features structurally by modeling adoption and valuation as a coupled equilibrium system with regime-dependent incentives, formulated as a Filippov differential inclusion. Token prices are determined endogenously through market clearing between usage-driven demand and regime-dependent speculative demand. We establish global well-posedness and identify conditions under which valuation thresholds become attracting manifolds. In these regimes, prices remain anchored at the threshold while adoption continues to evolve, generating persistent valuation plateaus and path dependence. When threshold crossings are regular and the induced dynamics are uniformly dissipative, endogenous boom–bust cycles are ruled out. The framework yields design-relevant insights for digital platforms. Valuation anchoring and volatility depend on governance primitives such as effective circulating supply and regime-dependent speculative depth. A diagnostic numerical analysis links time-at-anchor and sliding intensity to adoption volatility and platform risk, providing empirically interpretable indicators of stability in tokenized platforms.

Keywords: dynamic token valuation; discontinuous adoption dynamics; filippov differential inclusions; network effects; nonsmooth dynamical systems; sliding modes; speculative behavior; cryptocurrency volatility; stability analysis; behavioral finance; threshold switching; nonlinear feedback; platform economics

1. Introduction

Digital platforms are a dominant organizational form in the contemporary economy, shaping how value is created, coordinated, and governed. Beyond technological artefacts, platforms operate as economic institutions in which architecture, pricing rules, token design, and governance arrangements jointly determine incentives and beliefs among heterogeneous participants [5]. Platform outcomes therefore depend not only on technological performance, but on the interaction between participation decisions, market valuation, and institutional credibility.

A central insight of platform economics is that prices in platform environments are not merely market-clearing instruments but coordination devices. In two-sided markets, price *structure* rather than price *level* determines participation and ecosystem depth [32,33]. Subsequent work shows that pricing, adoption, and ecosystem expansion co-evolve dynamically [44,48], and that platform prices shape developer entry, user participation, and innovation incentives [31]. In these settings, valuation feeds back into participation expectations.

Tokenized and blockchain-based platforms intensify this feedback. In decentralized ecosystems, trust and coordination are mediated through a tradable token whose price simultaneously reflects usage demand, governance credibility, and speculative beliefs. The *unity* property identified by [29] formalizes this dual role: the same token prices access to services and incentivizes infrastructure

 doi:10.20944/preprints202603.1720.v1

provision. Related equilibrium models show that adoption, security provision, and valuation are jointly determined [6,10]. Empirical evidence confirms that usage, staking, and network activity are capitalized into token prices [23,29].

However, existing models largely assume smooth adjustment. Participation and valuation evolve continuously, and regime changes occur through parameter shifts or exogenous shocks. This smoothness assumption is analytically convenient but increasingly at odds with observed platform dynamics. Empirically, token markets display prolonged valuation plateaus, price clustering near salient levels, abrupt participation reversals, and weak short-run correlations between usage and price [24,27]. Adoption can continue to evolve materially while prices remain nearly constant. Such patterns suggest that platforms operate in coordination environments where incentives are revised discretely once credibility or sustainability thresholds are crossed [8,25].

This paper develops an equilibrium theory of tokenized platforms in which valuation thresholds are *structural coordination objects*. We show that when participation incentives switch discontinuously at a governance-sensitive valuation threshold P_c, the global geometry of platform dynamics changes qualitatively. The key mechanism is a feedback loop unique to tokenized platforms:

$$\text{Adoption} \;\rightarrow\; \text{Usage demand} \;\rightarrow\; \text{Token price} \;\rightarrow\; \text{Credibility and participation response.}$$

Because price is both a market outcome and a public coordination signal, a threshold in valuation becomes a threshold in participation incentives. Governance levers—issuance paths, effective circulating supply, lockups, staking constraints, and regime-dependent speculative depth—determine how the system behaves near that threshold.

Formally, we model adoption and valuation as a piecewise-smooth equilibrium system in which behavioral responsiveness changes discretely when P crosses P_c. The resulting dynamics are represented as a Filippov differential inclusion [12,16]. This framework accommodates abrupt re-optimization while preserving well-defined forward trajectories and economically meaningful state constraints. The model yields three qualitatively distinct regimes:

1. **Valuation anchoring:** the threshold P_c becomes an attracting manifold. Prices remain pinned at P_c while participation continues to evolve.
2. **Regime switching:** trajectories cross the threshold repeatedly, potentially generating endogenous boom–bust dynamics.
3. **Governance stabilization:** appropriate supply and responsiveness conditions eliminate cycles and restore convergence.

Anchoring arises when transactional demand and regime-dependent speculative support offset exactly at the threshold. We derive an explicit *anchoring window* (a_-, a_+) in participation space for which P_c is attracting. Its width depends directly on governance parameters such as effective supply $\bar{S}$ and regime asymmetry (β_L, β_R). In particular, comparative statics show that changes in circulating supply or speculative depth shift and reshape the anchoring interval, providing a direct link between governance design and valuation stability.

This mechanism differs fundamentally from existing token valuation models. Whereas prior frameworks characterize equilibrium prices under smooth adjustment, we characterize the *global phase geometry* of participation–valuation dynamics under discontinuous incentive revision. The resulting phenomena—valuation plateaus, sliding along credibility thresholds, and geometry-driven fragility—cannot arise in smooth models without exogenous shocks.

The paper makes three contributions to the platform literature. First, it introduces threshold-based discontinuities as structural equilibrium features of tokenized platforms, yielding a globally well-posed nonsmooth dynamical system. Second, it characterizes how governance parameters determine the qualitative regime of the ecosystem—anchored, switching, or stabilized—thereby linking token supply rules and market design directly to dynamic stability. Third, it proposes operational diagnostics, such as the share of time spent in attracting sliding ("time at anchor"), that can be measured using price

 doi:10.20944/preprints202603.1720.v1

and participation data. These diagnostics provide a bridge between platform governance design and empirically observable stability patterns.

While motivated by blockchain platforms, the mechanism is more general. Any digital platform in which valuation functions as a public coordination signal and incentives adjust discretely at salient thresholds can exhibit similar regime-dependent dynamics.

The remainder of the paper proceeds as follows. Section 2 develops the platform ecosystem model. Section 3 presents the analytical results. Section 4 interprets governance and stability implications. Section 5 concludes. Technical proofs and numerical diagnostics are provided in the appendices.

2. The Platform Ecosystem Model

We model a token-governed digital platform as a governance system that jointly determines ecosystem participation, token valuation, and incentive structure. The platform is not treated as a passive technology but as an institutional architecture in which protocol design, supply policy, and market access rules shape how participants coordinate and create value.

The ecosystem consists of three tightly coupled layers. First, a network of participants whose engagement exhibits complementarities (developer entry, validator support, user adoption) and congestion (blockspace limits, governance overhead, fee pressure). Second, a protocol-level token economy that encodes access rights, staking commitments, vesting rules, and supply discipline. Third, a token market that aggregates usage demand and portfolio demand into a publicly observed valuation signal.

Let $a_i(t) \in [0,1]$ denote participant i's engagement intensity and let $P(t) > 0$ denote the endogenous token price. Participation generates transactional demand for tokens, while governance-controlled supply and market-access conditions shape speculative demand. The resulting valuation feeds back into participation incentives through fee exposure, collateral requirements, and credibility perceptions. Adoption and valuation therefore co-evolve as equilibrium outcomes of platform design.

A central feature of tokenized platforms is that behavioral responsiveness changes at salient valuation milestones. When price crosses a credibility or sustainability threshold P_c, participants revise engagement heuristics and market depth can shift discretely. The threshold P_c represents a governance-sensitive coordination object, influenced by issuance schedules, lockups and vesting cliffs, staking requirements, listing access, disclosure commitments, security audits, or compliance milestones.

The joint evolution of $(a(t), P(t))$ is therefore modeled as a piecewise-smooth equilibrium system. We formalize regime switching at P_c as a Filippov differential inclusion [1,11,12,15,16]. This representation allows abrupt re-optimization induced by governance and market-design changes while preserving globally coherent equilibrium paths within and across regimes.

2.1. Platform Participants, Ecosystem Architecture, and Adoption

A tokenized platform coordinates a heterogeneous ecosystem of participants: end-users, developers, validators, liquidity providers, and integrators. Let $i \in \{1, \dots, N\}$ index these actors. Each participant chooses an engagement intensity $A_i(t) \in [0,1]$, interpreted as effective platform reliance: active usage, staking commitment, developer contribution, integration depth, or transactional dependence. The state A_i summarizes repeated participation decisions relative to outside opportunities.

Ecosystem architecture and complementarities.

Platform architecture shapes how participants benefit from one another. Interoperability, communication channels, governance exposure, and complementor linkages are represented by a weighted directed network $G = (V, E)$ with influence weights $w_{ij} \geq 0$. Let $W = (w_{ij})$ denote the adjacency matrix and define the local complementor-activity index

$$S_i(A) = \sum_{j=1}^{N} w_{ij} A_j, \qquad A \in [0,1]^N. \tag{1}$$

 doi:10.20944/preprints202603.1720.v1

Expression (1) captures ecosystem complementarities: developer entry increases user value, validator participation strengthens security, and liquidity provision improves transaction efficiency. Platform design enters exclusively through W, which reflects governance structure, protocol interoperability, and communication architecture. To ensure bounded exposure, we impose uniformly bounded outgoing influence,

$$\bar{w} = \max_{1 \le i \le N} \sum_{j=1}^{N} w_{ij} < \infty, \tag{2}$$

so $S_i(A) \in [0, \bar{w}]$ for all feasible states.

Participation value and governance channels:

Participant i's net platform value is

$$V_i(A, P) = \beta_i + \theta S_i(A) - \xi c(\bar{A}) - \chi u(P), \tag{3}$$

where aggregate ecosystem engagement is

$$\bar{A} = \frac{1}{N} \sum_{i=1}^{N} A_i. \tag{4}$$

Each term in (3) corresponds to a platform design channel. The baseline term β_i captures heterogeneous fit, capabilities, or alignment with platform purpose. The complementarity term $\theta S_i(A)$ links individual incentives to ecosystem exposure via (1), formalizing network effects central to platform theory. The congestion term $\xi c(\bar{A})$ depends on aggregate load (4) and captures scalability limits: blockspace congestion, fee pressure, governance coordination costs, or attention constraints. Improvements in throughput or governance efficiency shift this channel. The valuation-mediated term $u(P)$ captures how token valuation feeds back into participation. Higher P can increase effective participation costs through fee exposure, collateral requirements, staking opportunity costs, regulatory compliance burdens, or perceived systemic risk. Through (3), tokenomics and market outcomes directly influence ecosystem engagement.

Dynamic adjustment and regime dependence.

Engagement evolves according to

$$\dot{A}_i = A_i(1 - A_i)\Gamma_k\big(V_i(A, P)\big), \tag{5}$$

where $k \in \{L, R\}$ indexes the valuation regime. Equation (5) embeds the participation index (3) into a bounded adjustment rule. The normalization $\Gamma_k(0) = 0$ makes $V_i(A, P) = 0$ the indifference locus. The logistic factor ensures $A_i \in [0, 1]$ and reflects gradual strengthening or weakening of reliance rather than instantaneous entry or exit. Regime dependence arises through a governance-salient valuation threshold $P_c > 0$,

$$k = \begin{cases} L, & P < P_c, \\ R, & P > P_c. \end{cases} \tag{6}$$

Crossing P_c represents a discrete revision of participation heuristics and market conditions. In practice, such thresholds correspond to audit completion, compliance milestones, decentralization targets, security events, or sustainability reassessments that alter perceived platform viability. The adjustment functions satisfy

$$\Gamma_L'(v) \ge \Gamma_R'(v) \ge 0 \quad \text{a.e. } v \in \mathbb{R}, \qquad \Gamma_L \not\equiv \Gamma_R, \tag{7}$$

so marginal responsiveness is weaker in the high-valuation regime. Combined with (3), this captures environments in which elevated valuation amplifies congestion, collateral constraints, or regulatory scrutiny, dampening incremental engagement. For each fixed regime k, the vector field defined by

 doi:10.20944/preprints202603.1720.v1

(5) is locally Lipschitz on $[0,1]^N \times (0,\infty)$. Together with bounded exposure in (2), this prepares the ground for the global well-posedness result in Theorem 1.

2.2. Platform Governance, Token Market Design, and Valuation Dynamics

Token valuation in a decentralized platform is not an exogenous market outcome. It is jointly shaped by governance-controlled supply, ecosystem-generated usage demand, and market-access conditions that determine speculative depth.

Governance-controlled effective supply:

Let $\bar{S} > 0$ denote the *effective circulating supply* of tokens available for trade. This quantity reflects platform design choices, including issuance schedules, vesting cliffs, lockups, staking lock requirements, treasury releases, and listing or custody constraints. Although treated as fixed over the horizon studied, $\bar{S}$ is a direct governance lever. Through the market-clearing mechanism defined below, changes in $\bar{S}$ alter equilibrium valuation regimes.

Demand decomposition and regime dependence:

Total token demand combines ecosystem usage and portfolio demand,

$$D(A,P) = D_U(A,P) + D_{S,k}(P), \qquad k \in \{L,R\}, \tag{8}$$

where regime dependence follows the valuation rule (6).

Transactional demand: Usage demand arises from ecosystem engagement and scales with aggregate participation $\bar{A}$ defined in (4),

$$D_U(A,P) = \alpha\, \bar{A}\, \ell(P), \qquad \alpha > 0. \tag{9}$$

The function $\ell(P)$ is C^1, strictly decreasing, and satisfies $\lim_{P\to\infty} \ell(P) = 0$. It captures how valuation translates into effective participation cost. Higher token price increases fee exposure, collateral requirements, staking opportunity cost, or required token holdings per unit of activity. Through (9) and the adoption dynamics (5), platform engagement generates endogenous token demand.

Speculative and liquidity demand. Speculative demand reflects portfolio holding, security incentives, and liquidity provision,

$$D_{S,k}(P) = \beta_k\, s(P), \qquad k \in \{L,R\}. \tag{10}$$

The function $s(P)$ is C^1 and strictly decreasing, representing downward-sloping asset demand around perceived fundamental or collateral value. The regime parameter β_k scales effective market depth. We assume

$$\beta_L > \beta_R > 0, \tag{11}$$

so speculative support is stronger in the low-valuation regime. Economically, crossing the credibility threshold P_c may tighten collateral constraints, reduce risk appetite, alter liquidity provision, or trigger compliance-related restrictions, thereby reducing effective speculative depth. Through (11) and (6), valuation itself reshapes market liquidity, introducing a second feedback channel.

Token market adjustment:

Market clearing operates through an excess-demand adjustment rule,

$$g_k(A,P) = \kappa_P \Big[\alpha\, \bar{A}\, \ell(P) + \beta_k s(P) - \bar{S}\Big], \qquad \kappa_P > 0. \tag{12}$$

Price evolves according to

$$\dot{P} = g_k(A,P), \qquad k = \begin{cases} L, & P < P_c, \\ R, & P > P_c. \end{cases} \tag{13}$$

 doi:10.20944/preprints202603.1720.v1

The parameter κ_P captures token-market microstructure: order-book depth, arbitrage capital speed, market-maker inventory tolerance, and the responsiveness of liquidity providers. Equation (13) formalizes valuation as a coordination signal that aggregates ecosystem demand and governance-controlled supply. Together with the adoption dynamics (5), (13) closes the participation–valuation feedback loop central to platform theory.

Regime-wise equilibrium valuation:

For fixed $\bar{A}$ and regime k, the regime-specific clearing price $P_k^*(\bar{A})$ solves

$$\alpha\, \bar{A}\, \ell(P) + \beta_k s(P) = \bar{S}. \tag{14}$$

Because $\ell'(P) < 0$ and $s'(P) < 0$, the left-hand side of (14) is strictly decreasing in P, so $P_k^*(\bar{A})$ is unique whenever demand at $P \downarrow 0$ exceeds supply. Implicit differentiation of (14) yields

$$\frac{dP_k^*(\bar{A})}{d\bar{A}} = \frac{\alpha\, \ell(P_k^*(\bar{A}))}{-\alpha\, \bar{A}\, \ell'(P_k^*(\bar{A})) - \beta_k s'(P_k^*(\bar{A}))} > 0.$$

Within each regime, higher participation raises valuation. Combined with (3), valuation feeds back into participation incentives, establishing the endogenous coordination loop[1].

2.3. Filippov Formulation and Valuation Anchoring

The valuation threshold P_c introduced in (6) represents a governance-salient coordination level at which both participation heuristics and market depth can change discretely. Because regime selection depends directly on the token price, the joint adoption–valuation system (5)–(13) is inherently piecewise smooth. Let

$$x = (A_1, \ldots, A_N, P) \in \mathcal{X} := [0,1]^N \times (0, \infty),$$

where participation evolves according to (5) and valuation according to (13). Define the switching function

$$h(x) := P - P_c,$$

so that the switching manifold induced by governance rule (6) is

$$\Sigma := \{x \in \mathcal{X} : h(x) = 0\} = \{P = P_c\}.$$

For each regime $k \in \{L, R\}$, define the regime-specific vector field

$$f^{(k)}(x) = \begin{pmatrix} F_k(A, P) \\ g_k(A, P) \end{pmatrix},$$

where $F_k(A, P)$ is determined by the engagement dynamics (5) and $g_k(A, P)$ by the excess-demand rule (12). The vector field therefore combines: (i) ecosystem participation incentives driven by (3), and (ii) token-market adjustment driven by (8). Because regime selection in (13) depends discontinuously on P, valuation milestones induce structural shifts in incentives. We formalize this regime switching using the Filippov set-valued map $F : \mathcal{X} \rightrightarrows \mathbb{R}^{N+1}$,

$$F(x) = \begin{cases} \{f^{(L)}(x)\}, & h(x) < 0, \\ \mathrm{co}\{f^{(L)}(x), f^{(R)}(x)\}, & h(x) = 0, \\ \{f^{(R)}(x)\}, & h(x) > 0, \end{cases} \tag{15}$$

[1] The assumption $s'(P) < 0$ ensures regime-wise uniqueness of (14). Allowing $s'(P) > 0$ locally would capture momentum or trend-following demand, potentially generating self-reinforcing price dynamics within regimes. We maintain monotonicity to isolate threshold-driven coordination effects induced by governance and supply design.

 doi:10.20944/preprints202603.1720.v1

where co denotes the convex hull. A Filippov solution is an absolutely continuous trajectory $x(\cdot)$ satisfying

$$\dot{x}(t) \in F(x(t)) \quad \text{for almost every } t \geq 0.$$

Governance geometry at the credibility threshold:

At points $x \in \Sigma$, the outward normal to the switching manifold is

$$\nabla h = (0, \ldots, 0, 1),$$

so the normal component of the regime vector field is

$$\nabla h \cdot f^{(k)}(x) = g_k(A, P).$$

From (12), the sign of this component is determined by excess demand in the token market. A point $x \in \Sigma$ belongs to an *attracting sliding region* if

$$g_L(A, P_c) > 0 \quad \text{and} \quad g_R(A, P_c) < 0. \tag{16}$$

Condition (16) means that below the threshold the excess-demand rule pushes valuation upward, while above the threshold it pushes valuation downward. Both regimes therefore direct trajectories toward the governance-defined level P_c. When (16) holds, Filippov trajectories remain on Σ for nontrivial time intervals. Along such segments, $P(t) \equiv P_c$ and (13) implies $\dot{P} = 0$, while participation continues to evolve according to (5).

Valuation anchoring as a governance outcome:

Sliding on Σ corresponds to valuation anchoring. From (12), $g_k(A, P_c) = 0$ implies that total token demand in (8) exactly equals effective circulating supply $\bar{S}$ at the credibility threshold. Transactional demand generated by engagement through (9) and regime-dependent speculative depth through (10) offset precisely.

In this configuration, governance-defined valuation acts as a coordination anchor. Market valuation remains fixed at P_c even though ecosystem participation and network exposure continue to adjust via (5). Anchoring therefore emerges endogenously from the interaction between supply design, liquidity structure, and engagement incentives, providing a structural explanation for valuation plateaus observed in tokenized platform ecosystems.

2.4. Planar Mean-Field Reduction

Platform governance and market observers rarely monitor participant-level diffusion paths. Instead, they track aggregate ecosystem health through dashboard variables such as active users, transaction counts, developer activity, staked share, or total value secured. To align the analytical framework with this governance perspective, we adopt a planar mean-field reduction of the full network system defined by (5) and (13). We summarize ecosystem participation by a single state variable

$$a(t) \in [0, 1],$$

interpreted as average platform engagement, that is, the mean of A_i in (4). The reduction corresponds to a homogeneous-mixing approximation in which local exposure in (1) is replaced by its population-average effect, and heterogeneity in baseline propensities β_i and network weights w_{ij} is summarized by aggregate parameters. Economically, this shift moves the object of analysis from micro-level diffusion to ecosystem-level coordination, regime transitions, and stability of platform valuation. Such mean-field representations are standard in platform and network economics when global feedback and governance-relevant comparative statics dominate fine-grained topology.

Crucially, the structural mechanisms encoded in (3) are preserved. Network complementarities appear as scale effects, congestion as aggregate load, valuation-mediated participation costs through

 doi:10.20944/preprints202603.1720.v1

$u(P)$, and governance-induced regime shifts through (6). Under this reduction, aggregate engagement evolves according to

$$\dot{a} = a(1-a)\,\Gamma_k\big(V(a,P)\big), \qquad a \in [0,1], \tag{17}$$

which is the aggregate counterpart of (5). The reduced participation index becomes

$$V(a,P) = \bar{\beta} + \theta a - \xi c(a) - \chi u(P), \tag{18}$$

obtained from (3) by replacing $S_i(A)$ and $\bar{A}$ with a. Expression (18) preserves the four governance-relevant incentive channels: baseline ecosystem fit $\bar{\beta}$, scale-based complementarities θa, congestion and scalability limits $c(a)$, and valuation-mediated frictions $u(P)$. The logistic factor in (17) maintains $a \in [0,1]$ and guarantees forward invariance, ensuring that engagement remains economically admissible.

Token valuation continues to evolve through the governance-controlled excess-demand rule

$$\dot{P} = g_k(a,P) = \kappa_P \Big[\alpha\, a\, \ell(P) + \beta_k s(P) - \bar{S}\Big], \tag{19}$$

which is the aggregate counterpart of (12). Here $\bar{S}$ represents effective circulating supply, β_k regime-dependent liquidity depth, and κ_P token-market responsiveness. Together, (17) and (19) form a closed two-dimensional adoption–valuation feedback system, in which governance design, market liquidity, and ecosystem participation co-determine equilibrium paths. Regimes are governed by the credibility threshold

$$k = \begin{cases} L, & P < P_c, \\ R, & P > P_c, \end{cases} \tag{20}$$

inducing the switching manifold

$$\Sigma = \{(a,P) \in [0,1] \times (0,\infty) : P = P_c\}.$$

The planar system therefore inherits the piecewise structure formalized in (15). The planar model retains the structural levers that matter for platform design: effective supply $\bar{S}$, regime-dependent liquidity (β_L, β_R), and the credibility threshold P_c. It provides a transparent analytical laboratory for studying how governance choices reshape valuation anchoring, regime transitions, and global stability. Because the system (17)–(19) is two-dimensional, its geometry can be fully characterized. This permits precise classification of: regular crossing, valuation anchoring through sliding, endogenous boom–bust cycles, and stabilization through dissipativity, all in terms of platform design parameters.

3. Platform Model Analysis and Results

This section develops the central analytical results for the platform ecosystem model introduced in Section 2 and reduced to the planar adoption–valuation system (17)–(19) in Subsection 2.4. The objective is not merely to study a discontinuous dynamical system, but to classify the qualitative equilibrium regimes of a token-governed platform as functions of its structural design primitives.

The key primitives are: network complementarities and congestion embedded in (18), governance-determined circulating supply $\bar{S}$, regime-dependent speculative depth (β_L, β_R), and the credibility threshold rule (20). Together these elements determine how participation and valuation co-evolve when incentives adjust discretely at a salient valuation level. The analysis is conducted on the state space

$$\Omega = [0,1] \times (0,\infty),$$

where aggregate engagement a evolves according to (17) and valuation P according to (19). Regime switching occurs along the governance-defined manifold

$$\Sigma = \{(a,P) \in \Omega :\ P = P_c\},$$

 doi:10.20944/preprints202603.1720.v1

which inherits the piecewise structure induced by (20) and formalized through the Filippov construction (15). The results proceed in four steps. Each theorem isolates a distinct geometric property of (17)–(19) and translates it into a platform-relevant equilibrium regime.

Theorem 1 establishes global well-posedness and forward invariance. It shows that the discontinuous equilibrium system admits global Filippov solutions that remain in the economically meaningful domain Ω. Hence the governance rule (20) does not produce pathological trajectories, explosive behavior, or economically inadmissible states. This result provides the foundational feasibility of the platform model. Theorem 2 characterizes when the switching manifold Σ becomes an attracting sliding region. Under explicit inequalities on the excess-demand function (19), valuation remains pinned at P_c while participation continues to evolve. In platform terms, the credibility threshold acts as an endogenous coordination anchor. Price plateaus emerge structurally from the interaction of usage demand, speculative asymmetry, and governance-controlled supply. Theorem 3 identifies the alternative geometry in which the same threshold generates persistent oscillations. If a compact trapping region straddles Σ and neither regime contains stabilizing equilibria, the piecewise system (17)–(19) supports nonsmooth periodic orbits. Boom–bust cycles therefore arise endogenously from threshold-induced regime switching rather than from exogenous shocks. This theorem formalizes threshold-driven fragility in platform ecosystems. Theorem 4 provides design conditions that eliminate such cycles. Regular crossing at Σ combined with regime-wise dissipativity excludes periodic orbits and restores convergence. Economically, this translates into restrictions on $\bar{S}$, (β_L, β_R), and participation responsiveness in (17) that prevent threshold-induced amplification. Platform governance therefore reshapes the global geometry of equilibrium dynamics. Taken together, the four theorems classify token-governed platforms into three qualitatively distinct regimes:

- anchoring regimes in which valuation thresholds coordinate expectations,
- fragility regimes in which thresholds organize endogenous volatility,
- stabilized regimes in which governance design restores convergence.

The classification is structural. Each regime is determined by platform primitives rather than exogenous shocks or behavioral assumptions. The geometry of (17)–(19) therefore provides a governance-relevant map from design choices to ecosystem outcomes. Proofs are provided in Section B. Section C illustrates how the analytical conditions manifest in simulated phase portraits, time-at-anchor statistics, and robustness diagnostics. The analytical results supply the structural foundation for interpreting those diagnostics as equilibrium phenomena rather than numerical artefacts. Before interpreting valuation thresholds as coordination devices or instability triggers, we first establish that the discontinuous equilibrium system is globally well defined. The next theorem provides this baseline result.

Theorem 1 (Global well-posedness and forward invariance (Filippov))**.** *Consider the planar switching system* (17)–(19) *on* $\Omega := [0,1] \times (0,\infty)$ *with regime rule* (20) *and switching manifold* $\Sigma = \{P = P_c\}$. *Assume:*

(i) Γ_L, Γ_R *are globally Lipschitz, strictly increasing, and satisfy* $\Gamma_k(0) = 0$;
(ii) $V(a,P)$ *is given by* (18) *with* $c \in C^1([0,1])$ *and* $u \in C^1((0,\infty))$ *such that* $u'(P) > 0$;
(iii) $\ell, s \in C^1((0,\infty))$ *in* (19) *are strictly decreasing and positive, and* $\beta_L > \beta_R > 0$;
(iv) $\lim_{P \downarrow 0} s(P) = +\infty$;
(v) there exists $P_{\max} > P_c$ *such that*

$$\alpha\, \ell(P_{\max}) + \beta_L s(P_{\max}) - \bar{S} < 0.$$

Then for every initial condition $(a(0), P(0)) \in \Omega$ *there exists a global absolutely continuous Filippov solution to* (17)–(19). *Moreover,*

$$\Omega_{\max} := [0,1] \times (0, P_{\max}]$$

is forward invariant.

 doi:10.20944/preprints202603.1720.v1

Theorem 1 establishes that the threshold-based platform model is economically coherent. Participation remains within the feasible adoption interval $[0,1]$ and token valuation remains bounded in $\Omega_{\max}$, so the participation–valuation system evolves entirely within the economically admissible region of the state space. In particular, the governance rule (20), which activates different incentive regimes when valuation crosses the credibility threshold P_c, does not generate explosive price paths, pathological switching behavior, or economically infeasible states.

From a platform-governance perspective, this result guarantees that embedding credibility thresholds into participation incentives and token market clearing preserves the internal consistency of the ecosystem. Mechanisms such as valuation-triggered incentive adjustments, supply lockups, or participation subsidies can therefore be modeled as regime-switching rules without destabilizing the equilibrium structure of the platform economy. The theorem thus provides the foundational validity of the framework: it ensures that the participation–valuation dynamics remain well-defined and interpretable, allowing the model to serve as a structurally coherent laboratory for studying regime-dependent platform dynamics and governance interventions.

Theorem 2 (Sliding interval and valuation anchoring)**.** *Assume the hypotheses of Theorem 1. Let the switching manifold be*

$$\Sigma := \{(a,P) \in \Omega : \ P = P_c\},$$

and define

$$g_k(a,P) = \kappa_P\big[\alpha a \ell(P) + \beta_k s(P) - \bar{S}\big], \qquad k \in \{L,R\}.$$

Set

$$a_- := \frac{\bar{S} - \beta_L s(P_c)}{\alpha\, \ell(P_c)}, \qquad a_+ := \frac{\bar{S} - \beta_R s(P_c)}{\alpha\, \ell(P_c)}.$$

Then $a_- < a_+$ and the attracting Filippov sliding region on Σ is

$$\Sigma_s = \{(a,P_c) \in \Sigma : \ a \in (a_-,a_+)\}.$$

In particular, Σ_s is nonempty whenever $(a_-,a_+) \cap (0,1) \neq \emptyset$. For any Filippov trajectory entering Σ_s, there exists a nontrivial time interval on which

$$P(t) \equiv P_c,$$

while $a(t)$ evolves according to the induced sliding dynamics.

Theorem 2 identifies the first qualitative regime of the platform economy: *valuation anchoring*. When the excess-demand terms in (19) satisfy

$$g_L(a,P_c) > 0 \quad \text{and} \quad g_R(a,P_c) < 0,$$

transactional demand and regime-dependent speculative demand offset the effective circulating supply $\bar{S}$ from opposite sides at the credibility threshold P_c. Under these conditions the switching manifold $\Sigma = \{P = P_c\}$ becomes attracting, so the system enters a sliding regime in which valuation remains pinned at P_c while participation continues to evolve according to (17).

Economically, the credibility threshold functions as an endogenous coordination anchor for market expectations. Prices stabilize at the threshold even though underlying platform engagement continues to adjust. The explicit anchoring interval (a_-,a_+) therefore measures the range of participation levels for which valuation plateaus can persist. The width of this interval is governed by platform design parameters. Effective circulating supply $\bar{S}$, speculative-demand asymmetry (β_L,β_R), and the responsiveness of usage demand $\ell(P)$ jointly determine whether anchoring arises and how persistent it becomes. Empirically, this regime corresponds to prolonged valuation plateaus combined with continued movement in participation proxies such as transaction activity, staking participation, or user engagement.

 doi:10.20944/preprints202603.1720.v1

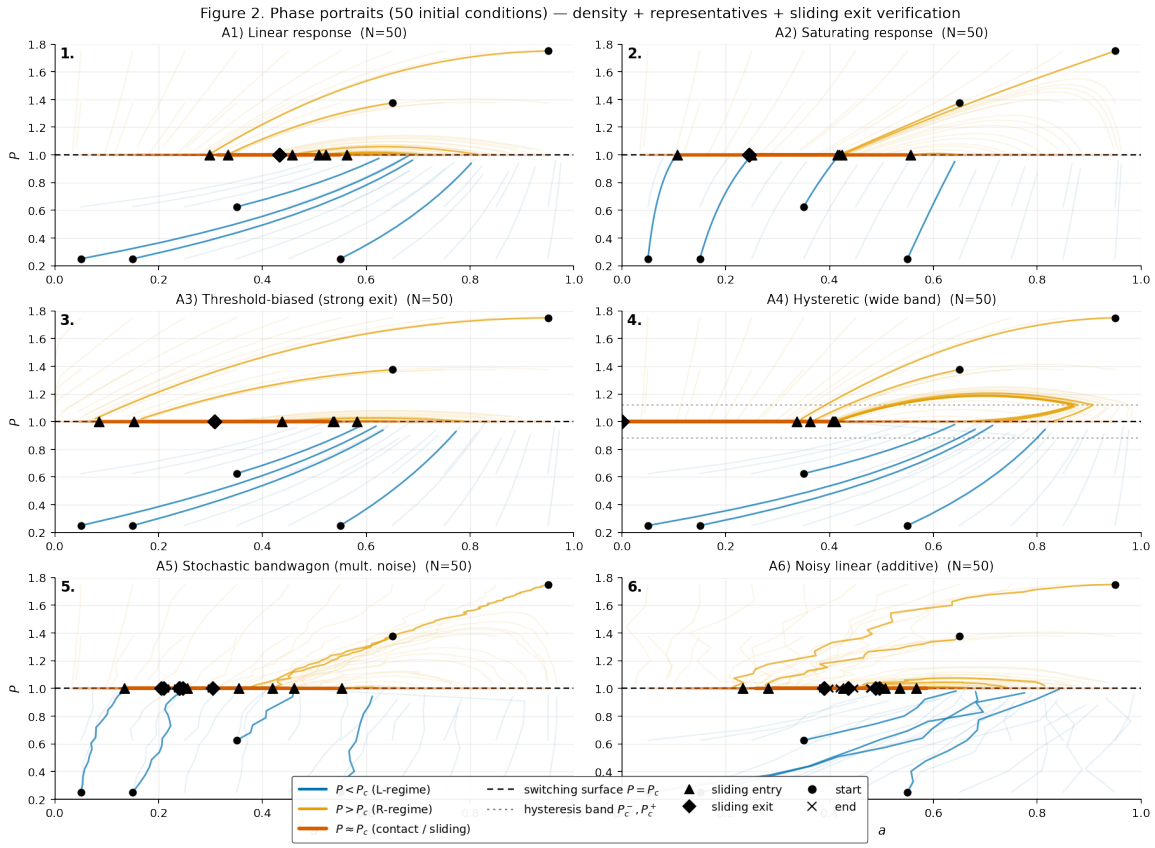

Figure 1. Phase portraits across 50 initial conditions (A1–A6). Trajectories converge toward $\Sigma = \{P = P_c\}$. Markers indicate entry and exit from sliding. Anchoring dominates under baseline parameters, consistent with Theorem 2.

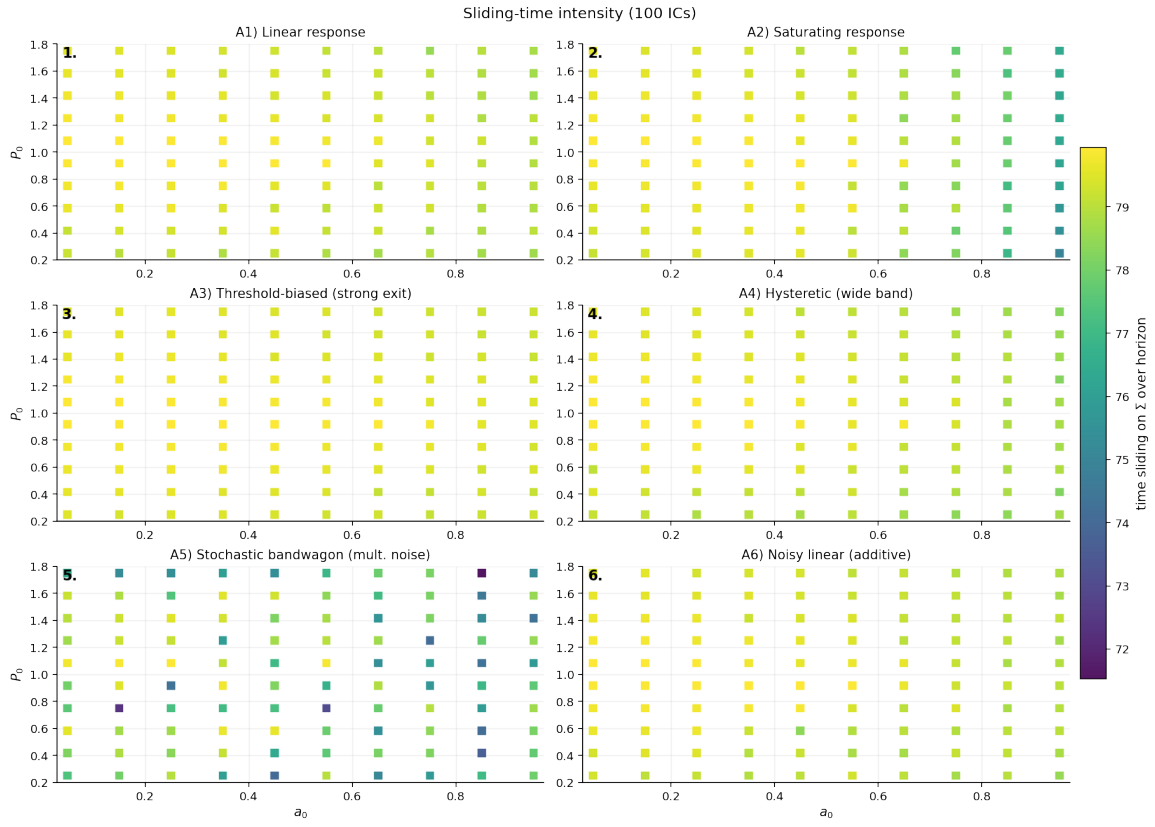

Figure 2. Sliding-time intensity across initial conditions (A1–A6). High sliding shares indicate persistent valuation anchoring. Results align with Theorem 2 and exclude sustained boom–bust dynamics in the baseline region.

 doi:10.20944/preprints202603.1720.v1

Theorem 3 (Existence of a nonsmooth limit cycle (boom–bust orbit)). *Assume the hypotheses of Theorem 1. Consider the associated planar Filippov inclusion $\dot{x} \in F(x)$ induced by (17)–(19) with switching manifold $\Sigma = \{(a, P) \in \Omega : P = P_c\}$.*

Suppose there exists a compact rectangle

$$\mathcal{R} = [a_1, a_2] \times [P_1, P_2] \subset \Omega, \qquad 0 < a_1 < a_2 < 1, \quad 0 < P_1 < P_c < P_2,$$

such that:

(i) ***Positive invariance.*** *$\mathcal{R}$ is positively invariant under the Filippov dynamics.*

(ii) ***Absence of stationary objects.*** *There are no equilibria of the smooth regime vector fields associated with (17)–(19) in $\mathcal{R} \setminus \Sigma$, and no pseudo-equilibria of the induced sliding dynamics on $\mathcal{R} \cap \Sigma$.*

(iii) ***Regular switching geometry.*** *For every $(a, P_c) \in \mathcal{R} \cap \Sigma$,*

$$g_L(a, P_c) \neq 0, \qquad g_R(a, P_c) \neq 0,$$

so each point is either a transversal crossing ($g_L g_R > 0$) or an attracting sliding point ($g_L > 0 > g_R$).

(iv) ***Non-Zeno regularity.*** *Filippov trajectories in $\mathcal{R}$ are forward unique and do not exhibit accumulation of switching times in finite time.*

Then the Filippov dynamics admit at least one periodic orbit contained in $\mathcal{R}$. Any such orbit intersecting Σ is piecewise smooth and nonsmooth at Σ, consisting of smooth regime segments connected by transversal crossings and possibly including attracting sliding arcs.

Theorem 3 identifies the second qualitative regime of the platform economy: *endogenous boom–bust dynamics*. If a compact trapping region straddles the credibility threshold and neither regime contains a stabilizing equilibrium, the regime-switching structure induced by (20) organizes recurrent oscillations in participation and valuation. In this configuration the system repeatedly crosses the threshold P_c, generating alternating phases of expansion and contraction in ecosystem activity.

Economically, the result shows that platform volatility can arise endogenously from governance-sensitive incentive switching rather than from external shocks. When participation incentives respond strongly to valuation signals but supply conditions and liquidity mechanisms fail to dampen the resulting adjustments, the participation–valuation system enters a self-sustained cycle. Observable indicators of this regime include repeated threshold crossings, clustered volatility in token valuation, and short-lived valuation plateaus.

Governance parameters determine whether such cycles persist. Adjustments to circulating supply $\bar{S}$, vesting and lockup structures, liquidity provisioning, or incentive responsiveness can increase system dissipativity and suppress the oscillatory regime, restoring convergence of participation and valuation.

Theorem 4 (Governance stabilization). *Assume the hypotheses of Theorem 1 and let $\Omega_{\max} = [0, 1] \times (0, P_{\max}]$ denote the forward-invariant set. Write the regime vector fields as*

$$f^{(k)}(a, P) = \begin{pmatrix} a(1-a)\Gamma_k(V(a,P)) \\ \kappa_P\left[\alpha a \ell(P) + \beta_k s(P) - \bar{S}\right] \end{pmatrix}, \qquad k \in \{L, R\},$$

with switching manifold $\Sigma = \{P = P_c\}$. Suppose:

(i) ***Regular crossing at the threshold.*** *For all $a \in [0, 1]$,*

$$g_L(a, P_c)\, g_R(a, P_c) > 0. \tag{21}$$

 doi:10.20944/preprints202603.1720.v1

A sufficient condition is

$$\bar{S} > \alpha\,\ell(P_c) + \beta_L s(P_c) \quad \text{or} \quad \bar{S} < \beta_R s(P_c). \tag{22}$$

(ii) ***Regime-wise differentiability.*** $\Gamma_L, \Gamma_R \in C^1(\mathbb{R})$ *with bounded derivatives.*

(iii) ***Uniform dissipativity.*** *There exists* $\eta > 0$ *such that for each* $k \in \{L, R\}$,

$$\operatorname{div} f^{(k)}(a, P) \le -\eta \quad \text{for all } (a, P) \in \Omega_{\max} \setminus \Sigma. \tag{23}$$

Then the Filippov system admits no periodic orbits in $\Omega_{\max}$. *Every* ω*-limit set intersects the set of Filippov equilibria. If all Filippov equilibria are isolated, every trajectory converges to an equilibrium and endogenous boom–bust oscillations are excluded.*

Theorem 4 identifies the third qualitative regime of the platform economy: *governance-stabilized convergence*. When trajectories cross the credibility threshold regularly, sliding along the switching manifold cannot persist. Combined with uniform dissipativity of the participation–valuation dynamics, this produces contraction of trajectories and eliminates self-sustained oscillations. From a governance perspective, this result shows that platform design can suppress endogenous boom–bust dynamics while preserving the coordination role of the credibility threshold. Key design parameters—effective circulating supply $\bar{S}$, liquidity asymmetry (β_L, β_R), and the responsiveness of participation in (17)—reshape the global phase geometry of the participation–valuation system. Through appropriate calibration of these mechanisms, governance can transform an oscillatory ecosystem into one that converges toward a stable participation–valuation equilibrium without removing the informational function of the threshold P_c.

This regime classification yields a governance-relevant taxonomy of platform dynamics. It links core structural primitives— participation complementarities and congestion embedded in (17) through (18), market-clearing and liquidity mechanisms in (19), and protocol design parameters such as effective circulating supply $\bar{S}$ and regime-dependent speculative depth (β_L, β_R)—to qualitatively distinct ecosystem outcomes. In the anchoring regime, characterized in Theorem 2, the valuation threshold $\Sigma = \{P = P_c\}$ becomes an attracting manifold. The excess-demand structure in (19) offsets circulating supply at P_c, so price remains pinned while participation continues to evolve under (17). Valuation stability therefore does not imply stability of usage or network organization. In the fragility regime, identified in Theorem 3, the same threshold rule (20) interacts with insufficient dissipativity in (17)–(19) to generate endogenous boom–bust cycles. Here the threshold acts as a switching amplifier rather than a coordination anchor. In the stabilized regime, characterized by Theorem 4, regular crossing at Σ together with regime-wise contraction eliminates periodic motion. Supply calibration and liquidity design reshape the geometry of (17)–(19) so that all trajectories converge to equilibrium. The realized regime is thus a structural consequence of design. Valuation thresholds can coordinate expectations, amplify volatility, or restore stability depending on how governance jointly calibrates circulating supply, speculative depth, and participation responsiveness.

4. Discussion

The equilibrium implications of the model arise from embedding discontinuous incentive adjustment directly into the adoption–valuation feedback system (17)–(19). Standard platform frameworks impose smooth adjustment, so regime changes occur only through large shocks or gradual parameter variation [9,28,33,37] Here, responsiveness switches discretely at the governance-sensitive threshold P_c defined in (20). Theorem 1 establishes that this piecewise structure admits global Filippov solutions that remain confined to the economically meaningful domain $\Omega_{\max}$, with formal barrier verification provided in Appendix B. As a result, qualitative behavior near the switching manifold $\Sigma = \{P = P_c\}$—including sliding, transversal crossing, and possible nonsmooth periodic motion—is a structural feature of equilibrium rather than a numerical artefact. This modeling choice reflects

 doi:10.20944/preprints202603.1720.v1

empirical evidence that users and investors revise participation and speculative demand abruptly when valuation crosses salient credibility thresholds [23,27,29].

The threshold P_c enters the system structurally through (20) and organizes the geometry of the excess-demand rule in (19). Its role as an endogenous coordination object is formalized in Theorem 2, which derives the sliding interval (a_-, a_+) explicitly. Because a_- and a_+ depend directly on effective circulating supply $\bar{S}$, speculative intensities (β_L, β_R), and the usage-demand channel $\ell(P_c)$, governance primitives determine whether the switching manifold becomes an attracting set. Issuance paths, lockups, staking rules, and liquidity design therefore reshape the geometry of Σ rather than merely shifting valuation levels. Empirical evidence that supply rules and market-access frictions affect volatility regimes [21,24] is consistent with this structural channel.

When $(a_-, a_+) \cap (0,1) \neq \emptyset$, Filippov trajectories entering Σ satisfy $P(t) \equiv P_c$ over nontrivial intervals while participation evolves according to (17). Valuation plateaus thus arise endogenously from the interaction of transactional demand, speculative asymmetry, and supply design. The numerical analysis in Appendix C illustrates this geometry. Phase portraits in Figure 1 and sliding-intensity heatmaps in Figure 2 show high sliding shares across adoption laws and initial conditions. Tables A2 and A3 confirm that anchoring occupies a substantial region of the baseline design space rather than a knife-edge configuration.

At the same time, anchoring of valuation does not imply uniformity of participation outcomes. Appendix A introduces alternative adjustment specifications capturing nonlinear saturation, exit asymmetry, hysteresis, and stochastic amplification. Even when $P(t)$ remains pinned at P_c, late-time adoption statistics differ across specifications (Table A3, Figure A2). The geometry of Σ governs valuation stability, while the microfoundations embedded in (17) govern participation levels.

Theorem 3 identifies conditions under which the same threshold rule (20) generates endogenous boom–bust cycles. When trajectories of (17)–(19) are confined to a compact trapping region that straddles Σ and neither regime contains a stabilizing equilibrium nor a stabilizing sliding pseudo-equilibrium, the piecewise structure alone can organize recurrent oscillations. The Filippov Poincaré–Bendixson argument in Appendix B formalizes this fragility window. Baseline simulations operate outside this configuration, as shown in Appendix C, where sliding dominance precludes trapping-region geometry.

Theorem 4 provides sufficient conditions—regular crossing at Σ and regime-wise dissipativity—to exclude periodic orbits. Uniform negative divergence of the regime vector fields associated with (17)–(19) yields a Filippov extension of the Bendixson criterion. Numerical illustrations confirm that when (21)– (23) hold, sliding intensity collapses and trajectories converge smoothly. Governance parameters therefore determine not only incentive levels but the global phase geometry of the participation–valuation system.

Taken together, Theorems 1– 4 show that valuation thresholds are structural equilibrium objects. They can anchor expectations, generate endogenous fragility, or restore convergence depending on how supply, liquidity, and responsiveness are calibrated. The appendices provide formal proofs and quantitative diagnostics for each mechanism. The framework thus yields a unified equilibrium account of threshold-driven coordination and instability in tokenized platforms.

5. Conclusion

This paper develops an equilibrium theory of tokenized platforms in which valuation thresholds act as structural coordination mechanisms. Participation incentives and speculative demand adjust endogenously when valuation crosses the governance-sensitive threshold P_c. Price therefore plays a dual role: it clears the token market while also serving as a public coordination signal that reshapes participation incentives through (17). Modeling this interaction as a Filippov differential inclusion captures discontinuous incentive adjustments while preserving global well-posedness and economically meaningful state constraints.

 doi:10.20944/preprints202603.1720.v1

The analysis shows that the credibility threshold P_c organizes the global geometry of participation–valuation dynamics. Three qualitative regimes emerge. First, when the sliding conditions of Theorem 2 hold, the threshold becomes an attracting manifold and valuation remains anchored at P_c while participation continues to evolve. Second, when dissipativity is insufficient, Theorem 3 shows that the same threshold-based switching rule can generate endogenous boom–bust cycles without exogenous shocks. Third, when regular threshold crossing combines with regime-wise contraction, Theorem 4 yields global convergence of the participation–valuation system.

These regimes correspond directly to governance design choices. Supply schedules, vesting and lockup structures, staking incentives, and liquidity conditions influence effective circulating supply $\bar{S}$ and speculative asymmetry (β_L, β_R), which jointly determine the geometry of the switching manifold. Through these mechanisms, governance can transform a fragile ecosystem into a stabilized one while preserving the coordination role of the valuation threshold.

The framework also provides observable diagnostics linking theory to practice. Statistics such as the time spent near the valuation anchor, plateau durations, and the frequency of regime transitions can be estimated from price series and participation proxies. These indicators allow platform designers to infer whether the system operates in an anchoring, fragility, or stabilized regime.

Several limitations clarify the scope of the framework. The model abstracts from micro-level strategic heterogeneity and represents participation through an aggregate adoption variable. In addition, the credibility threshold P_c and effective circulating supply $\bar{S}$ are treated as exogenous governance parameters, though in practice they may evolve through liquidity provision, regulation, or protocol decisions. Finally, the proposed diagnostics are not calibrated to a specific dataset. Future work may combine the present theoretical structure with empirical estimation using on-chain activity measures and liquidity data to identify threshold regimes in real platform ecosystems.

Despite these limitations, the central insight remains robust. Governance-sensitive valuation thresholds shape the global geometry of platform dynamics. Depending on how supply, liquidity, and incentive responsiveness are calibrated, the same threshold can anchor expectations, amplify volatility, or stabilize the participation–valuation system.

Appendix A. Adoption Update Specifications

Table A1 summarises the adoption update rules used in the numerical analysis. All rules share a common valuation-based switching mechanism at the threshold $P = P_c$ (or the band $[P_c^-, P_c^+]$ for A4), which represents a governance-relevant credibility threshold in the platform ecosystem. The alternative rules capture distinct platform design mechanisms. They allow controlled comparisons between (i) linear versus saturated adjustment in participation incentives, (ii) symmetric participation responses versus exit-biased dynamics arising from liquidity frictions or loss of confidence, (iii) instantaneous adjustment versus hysteresis generated by reputation, switching costs, or user memory, and (iv) multiplicative social noise reflecting network amplification versus additive idiosyncratic shocks. These design choices map directly into observable ecosystem outcomes. They are reflected in the diagnostics reported in Appendix C, including time spent at the valuation anchor, the frequency and duration of sliding episodes, late-time participation distributions, and basin geometry. Together, these diagnostics illustrate how alternative platform design choices influence the stability, fragility, or persistence of valuation coordination regimes.

doi:10.20944/preprints202603.1720.v1

Table A1. Adoption update specifications used in the simulations (A1–A6). Each rule defines an adoption drift (or stochastic differential) that is *regime-conditioned* on the valuation threshold: the governing regime switches at $P = P_c$ (or, for A4, within a two-threshold band). These specifications are chosen to be structurally distinct while remaining comparable: A1–A3 are deterministic benchmarks (linear, saturating, and exit-biased), A4 introduces genuine hysteresis and regime persistence, and A5–A6 introduce stochastic participation dynamics (multiplicative "bandwagon" noise versus additive idiosyncratic shocks). Together they allow controlled comparisons of how nonlinearity, asymmetry, memory, and stochasticity shape valuation anchoring (Filippov sliding), regime interaction, and basin geometry in the coupled adoption–valuation system.

ID	Name	Functional form	Platform interpretation
A1	Linear response	$\dot{a} = \begin{cases} \alpha_L(1-a), & P < P_c, \\ -\alpha_R a, & P > P_c \end{cases}$	**Baseline participation adjustment.** Representative participation increases linearly when valuation lies below the credibility threshold (entry/expansion region) and decays proportionally when valuation exceeds the threshold (contraction/exit region). This rule serves as a benchmark with monotone incentives and no saturation effects.
A2	Saturating response	$\dot{a} = \begin{cases} \alpha_L a(1-a), & P < P_c, \\ -\alpha_R a(1-a), & P > P_c \end{cases}$	**Endogenous saturation under ecosystem crowding.** Logistic adjustment captures diminishing marginal incentives near full participation (capacity limits, congestion, or diminishing incremental network benefits) and near zero participation (limited peer reinforcement). Relative to A1, the dynamics slow down near the boundaries even within the same valuation regime.
A3	Threshold-biased	$\dot{a} = \begin{cases} \alpha_L(1-a), & P < P_c, \\ -\alpha_R a - \beta, & P > P_c \end{cases}$	**Exit amplification above the threshold.** An additional negative drift $\beta > 0$ accelerates exit once valuation exceeds P_c, capturing loss sensitivity, trust breakdown, compliance frictions, or reputational cascades that make contraction sharper than expansion.
A4	Hysteretic (two-threshold)	$k(t^+) = \begin{cases} L, & P \le P_c^-, \\ R, & P \ge P_c^+, \\ k(t^-), & P_c^- < P < P_c^+, \end{cases}$ $\dot{a} = \begin{cases} \alpha_L(1-a), & k(t) = L, \\ -\alpha_R a, & k(t) = R \end{cases}$	**Regime persistence and path dependence.** Separate entry and exit thresholds ($P_c^- < P_c^+$) generate genuine hysteresis, representing persistence in user beliefs, switching costs, governance frictions, or delayed coordination. Within the band, the ecosystem "remembers" its last regime, so valuation changes need not immediately reverse participation incentives.
A5	Stochastic bandwagon	$da = \begin{cases} \alpha_L a(1-a)\,dt + \sigma a(1-a)\,dW_t, & P < P_c, \\ -\alpha_R a(1-a)\,dt + \sigma a(1-a)\,dW_t, & P > P_c \end{cases}$	**Social amplification under uncertainty.** Multiplicative noise captures endogenous dispersion in participation updates that grows with the "room to move" (i.e. strongest at intermediate adoption). This represents experimentation, peer-driven amplification, and endogenous uncertainty in ecosystem participation that interacts with valuation anchoring.
A6	Noisy linear	$da = \begin{cases} \alpha_L(1-a)\,dt + \sigma\,dW_t, & P < P_c, \\ -\alpha_R a\,dt + \sigma\,dW_t, & P > P_c \end{cases}$	**Idiosyncratic shocks around a linear benchmark.** Additive noise represents exogenous news shocks, heterogeneous idiosyncratic participation changes, or measurement noise. Relative to A5, uncertainty does not vanish at the boundaries, so small fluctuations can persist even near $a \approx 0$ or $a \approx 1$.

 doi:10.20944/preprints202603.1720.v1

Appendix B. Technical Analysis and Proofs

Proof of Theorem 1. We verify the hypotheses of standard existence results for Filippov differential inclusions (see [16, Ch. 2] and [1, Ch. 1]).

Step 1: Local regularity away from Σ. For $P \neq P_c$, the system coincides with one of the smooth vector fields $f^{(L)}$ or $f^{(R)}$. Because $V(a,P)$ is C^1 on Ω, Γ_k is globally Lipschitz, and ℓ, s are C^1 on $(0,\infty)$, each $f^{(k)}$ is locally Lipschitz on Ω. Classical ODE theory therefore guarantees local existence and uniqueness of solutions away from Σ.

Step 2: Filippov regularization on Σ. On the switching manifold $\Sigma = \{P = P_c\}$, the Filippov set-valued map

$$F(x) = \mathrm{co}\{f^{(L)}(x), f^{(R)}(x)\}$$

is upper semicontinuous with nonempty compact convex values. Moreover, on every compact subset of $\Omega_{\max}$, both $f^{(L)}$ and $f^{(R)}$ are bounded, hence F is locally bounded. It follows from Filippov's existence theorem [16, Th. 1, p. 106] that for every initial condition in $\Omega_{\max}$ there exists at least one absolutely continuous trajectory satisfying $\dot{x}(t) \in F(x(t))$ almost everywhere.

Step 3: Forward invariance of $a \in [0,1]$. At the boundary points $a = 0$ and $a = 1$,

$$\dot{a} = a(1-a)\Gamma_k(V(a,P)) = 0,$$

for both regimes $k \in \{L, R\}$. Thus the vector field is tangent to the boundary, and standard viability arguments imply that trajectories cannot exit the interval $[0,1]$.

Step 4: Lower barrier for the price process. By assumption (iv) of Theorem 1,

$$\lim_{P \downarrow 0} s(P) = +\infty.$$

Since $\beta_k > 0$ and ℓ is bounded on $(0, P_c]$,

$$\alpha a \ell(P) + \beta_k s(P) - \bar{S} \longrightarrow +\infty \quad \text{as } P \downarrow 0,$$

uniformly in $a \in [0,1]$ and $k \in \{L, R\}$. Hence there exists $\delta > 0$ such that

$$\dot{P} > 0 \quad \text{whenever } 0 < P < \delta.$$

Therefore $P(t)$ cannot reach zero in finite time.

Step 5: Upper barrier for the price process. By assumption (v) of Theorem 1 and monotonicity of ℓ and s, for any $P \geq P_{\max}$ and any $a \in [0,1]$,

$$\alpha a \ell(P) + \beta_L s(P) - \bar{S} \leq \alpha \ell(P_{\max}) + \beta_L s(P_{\max}) - \bar{S} < 0.$$

Since $\beta_R < \beta_L$, the same inequality holds with β_R. Consequently,

$$\dot{P} < 0 \quad \text{whenever } P \geq P_{\max}.$$

Thus $P(t)$ cannot exceed $P_{\max}$ once inside $\Omega_{\max}$.

Step 6: Global existence. Because $a(t) \in [0,1]$ and $P(t) \in (0, P_{\max}]$ for all forward times, solutions remain in the compact forward-invariant set $\Omega_{\max}$. Local existence together with boundedness of the vector field implies that solutions extend to all $t \geq 0$.

□

Proof of Theorem 3. Fix an initial condition $x_0 \in \mathcal{R}$. By Theorem 1, there exists a global Filippov solution $x(\cdot)$ with $x(0) = x_0$.

 doi:10.20944/preprints202603.1720.v1

Step 1: Existence of a compact invariant ω-limit set. By positive invariance of $\mathcal{R}$, the trajectory satisfies $x(t) \in \mathcal{R}$ for all $t \geq 0$. Since $\mathcal{R}$ is compact, the forward orbit $\{x(t) : t \geq 0\}$ is precompact. Hence the ω-limit set

$$\omega(x_0) := \bigcap_{T>0} \overline{\{x(t) : t \geq T\}}$$

is nonempty, compact, connected, and invariant under the Filippov flow.

Step 2: Regularity of switching and absence of pathological behavior. By assumption (iii), each point of $\mathcal{R} \cap \Sigma$ is either a transversal crossing point ($g_L g_R > 0$) or belongs to an attracting sliding segment ($g_L > 0 > g_R$). In particular, there are no tangencies or two-fold singularities. Assumption (iv) excludes Zeno accumulation of switching times. Therefore Filippov trajectories in $\mathcal{R}$ are piecewise C^1 with finitely many switching events on each bounded time interval (see [12,16]).

Step 3: Exclusion of equilibria and reduction to periodic dynamics. By assumption (ii), there are:

- no equilibria of $f^{(L)}$ or $f^{(R)}$ in $\mathcal{R} \setminus \Sigma$, and
- no pseudo-equilibria of the sliding vector field on $\mathcal{R} \cap \Sigma$.

Hence $\omega(x_0)$ contains no equilibrium points. Moreover, because switching is regular and non-Zeno, the Filippov system on $\mathcal{R}$ satisfies the hypotheses of the planar Filippov Poincaré–Bendixson theorem (see [12]), which states that every nonempty compact invariant set without equilibria must be a periodic orbit. Therefore $\omega(x_0)$ is a periodic orbit contained entirely in $\mathcal{R}$.

Step 4: Nonsmooth structure of the orbit. If the periodic orbit intersects Σ, it consists of smooth segments governed by $f^{(L)}$ and $f^{(R)}$, connected by transversal switching points and possibly by sliding segments along Σ. Hence the orbit is piecewise smooth and nonsmooth at Σ.

□

Proof of Theorem 4. Suppose, for contradiction, that a periodic Filippov orbit $\gamma \subset \Omega_{\max}$ exists.

Step 1: Regular crossing geometry. By assumption (i) of Theorem 4,

$$g_L(a, P_c) g_R(a, P_c) > 0 \quad \text{for all } a \in [0, 1].$$

Hence Σ is a regular crossing manifold: no point on Σ is a sliding or tangency point. Therefore γ is a closed, piecewise C^1 curve that intersects Σ transversally a finite number of times (see [12]).

Step 2: Decomposition of the enclosed region. Let $D \subset \Omega_{\max}$ denote the compact region enclosed by γ. Decompose

$$D = D_L \cup D_R, \qquad D_L := D \cap \{P < P_c\}, \quad D_R := D \cap \{P > P_c\}.$$

On each D_k, the vector field $f^{(k)}$ is C^1. The boundary of D_k consists of: (i) the portion of γ lying in regime k, and (ii) transversal interface segments along Σ.

Step 3: Divergence integration. Applying Green's theorem on each D_k gives

$$\iint_{D_k} \operatorname{div} f^{(k)} \, dA = \oint_{\partial D_k} f^{(k)} \cdot n_k \, ds, \qquad k \in \{L, R\},$$

where n_k is the outward unit normal on ∂D_k. Summing over $k \in \{L, R\}$ yields

$$\iint_{D_L} \operatorname{div} f^{(L)} \, dA + \iint_{D_R} \operatorname{div} f^{(R)} \, dA = \oint_{\gamma} f \cdot n \, ds + \int_{\Sigma \cap D} \left(f^{(L)} - f^{(R)}\right) \cdot n_\Sigma \, ds.$$

Because γ is a periodic orbit, the vector field is tangent to γ almost everywhere, so $f \cdot n = 0$ on γ. Along Σ, assumption (i) guarantees regular crossing and absence of sliding. The outward normals of D_L and D_R along the interface are opposite, so the flux contributions across Σ cancel exactly. Therefore,

$$0 = \iint_{D_L} \operatorname{div} f^{(L)} \, dA + \iint_{D_R} \operatorname{div} f^{(R)} \, dA.$$

 doi:10.20944/preprints202603.1720.v1

Step 4: Dissipativity contradiction. By assumption (iii) of Theorem 4, there exists $\eta > 0$ such that

$$\operatorname{div} f^{(k)}(a,P) \le -\eta \quad \text{for all } (a,P) \in \Omega_{\max} \setminus \Sigma, \qquad k \in \{L,R\}.$$

Since D has positive Lebesgue measure,

$$\iint_{D_L} \operatorname{div} f^{(L)}\, dA + \iint_{D_R} \operatorname{div} f^{(R)}\, dA \le -\eta |D| < 0,$$

which contradicts the previous equality. Hence no periodic orbit exists in $\Omega_{\max}$.
Step 5: Asymptotic behavior. Compactness and forward invariance of $\Omega_{\max}$ imply that every Filippov trajectory admits a nonempty ω-limit set. In the absence of periodic orbits, the planar Filippov Poincaré–Bendixson alternative (see [12]) implies that every ω-limit set contains an equilibrium or pseudo-equilibrium. If equilibria are isolated, convergence is to a single equilibrium point.
□

Proof of Theorem 2. Define the switching function

$$h(a,P) = P - P_c,$$

so that the switching manifold is $\Sigma = \{(a,P) \in \Omega : h(a,P) = 0\}$ and

$$\nabla h(a,P) = (0,1).$$

For each regime $k \in \{L,R\}$, the normal component of the vector field at a point $(a,P_c) \in \Sigma$ is

$$\nabla h(a,P_c) \cdot f^{(k)}(a,P_c) = f_2^{(k)}(a,P_c) = g_k(a,P_c).$$

By the standard Filippov sliding criterion (see [16, Ch. 2] or [12]), Σ contains an attracting sliding region precisely at those points where the vector fields on either side point toward the manifold, i.e.

$$g_L(a,P_c) > 0 \quad \text{and} \quad g_R(a,P_c) < 0.$$

Because $\kappa_P > 0$ and $\ell(P_c) > 0$, these inequalities are equivalent to

$$\alpha a \ell(P_c) + \beta_L s(P_c) - \bar{S} > 0, \quad \text{and} \quad \alpha a \ell(P_c) + \beta_R s(P_c) - \bar{S} < 0.$$

Solving the first inequality yields

$$a > \frac{\bar{S} - \beta_L s(P_c)}{\alpha \ell(P_c)} =: a_-,$$

while the second yields

$$a < \frac{\bar{S} - \beta_R s(P_c)}{\alpha \ell(P_c)} =: a_+.$$

Since $\beta_L > \beta_R$ and $s(P_c) > 0$, we have

$$\bar{S} - \beta_L s(P_c) < \bar{S} - \beta_R s(P_c),$$

which implies $a_- < a_+$. Hence the attracting sliding region on Σ is

$$\Sigma_s = \{(a,P_c) \in \Sigma : a \in (a_-, a_+)\}.$$

The sliding region is nonempty whenever $(a_-, a_+) \cap (0,1) \neq \emptyset$. Finally, by the definition of Filippov solutions, if a trajectory reaches a point in Σ_s, the convexified vector field contains directions

 doi:10.20944/preprints202603.1720.v1

tangent to Σ whose normal component vanishes. The induced sliding vector field therefore keeps the trajectory on Σ for a nontrivial time interval (see [16]). Along such segments,

$$P(t) \equiv P_c,$$

which corresponds to a valuation plateau. □

Appendix C. Numerical Analysis

The numerical analysis examines how alternative platform design choices affect participation–valuation dynamics around the credibility threshold P_c. In the model, design primitives such as effective circulating supply $\bar{S}$, liquidity asymmetry (β_L, β_R), and the structure of participation incentives determine how the ecosystem responds when valuation approaches the threshold. The simulations therefore interpret different adoption rules as stylized governance mechanisms that shape user adjustment, network amplification, and market responsiveness. The diagnostics reported below—such as time spent at the valuation anchor, sliding episode persistence, exit patterns, and late-time participation distributions—illustrate how these design features influence whether the platform ecosystem exhibits anchoring, volatility, or stable convergence.

Table A2. Time allocation and state ranges for single-trajectory simulations (A1–A6). For each adoption law, the table reports the fractions of the horizon spent in the left regime ($P < P_c$), in attracting Filippov sliding on the valuation threshold $\Sigma := \{P = P_c\}$, and in the right regime ($P > P_c$), together with the observed ranges of adoption $a(t)$ and price $P(t)$. All quantities are computed from a single trajectory over horizon $T = 120$ (fixed step size) using the sliding and contact definitions described in this appendix.

Law	T_L/T	$T_\Sigma^{\text{slide}}/T$	T_R/T	$a_{\min}$–$a_{\max}$	$P_{\min}$–$P_{\max}$
A1) Linear response	0.0025	0.9965	0.0010	0.250–0.633	0.550–1.002
A2) Saturating response	0.0032	0.9968	$< 10^{-4}$	0.245–0.329	0.550–1.000
A3) Threshold-biased (strong exit)	0.0026	0.9973	0.0002	0.250–0.595	0.550–1.001
A4) Hysteretic (wide band)	0.0025	0.9855	0.0121	$< 10^{-6}$–0.871	0.550–1.184
A5) Stochastic bandwagon (mult. noise)	0.0032	0.9968	$< 10^{-4}$	0.153–0.380	0.550–1.001
A6) Noisy linear (additive)	0.0026	0.9973	0.0001	0.247–0.592	0.550–1.001

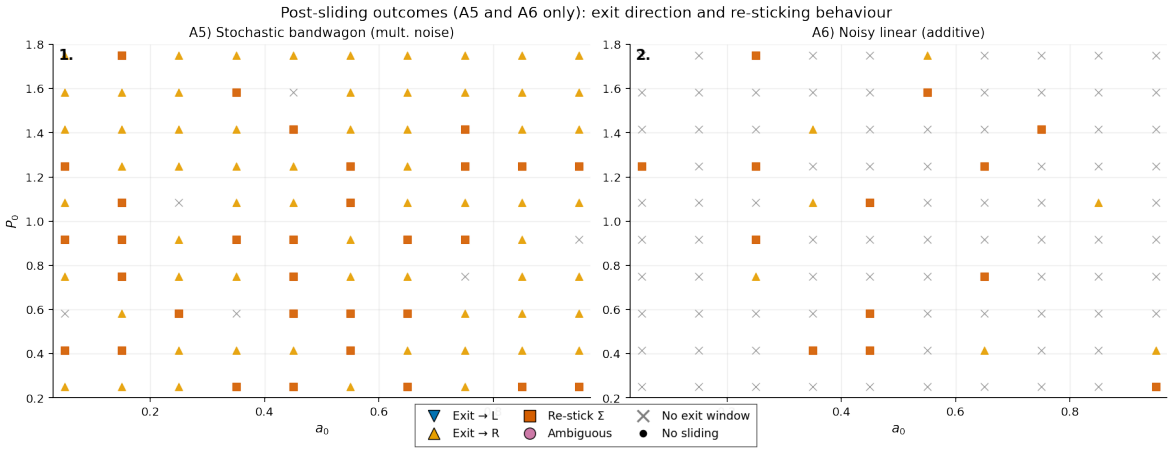

Figure A1. Post-sliding outcomes under stochastic adoption (A5 and A6): exit direction and re-anchoring. For each initial condition, the first detected attracting sliding episode on Σ is identified, if it exists. Subsequent behavior is classified over a fixed post-window after the episode ends as *Exit to L* if $P < P_c - \text{tol}_{\text{contact}}$, *Exit to R* if $P > P_c + \text{tol}_{\text{contact}}$, *Re-stick* Σ if the trajectory remains within the contact band for at least 85% of the post-window, and *Ambiguous* otherwise. Initial conditions with no detected sliding are labelled *No sliding*, and cases where the episode ends too close to the horizon are labelled *No exit window*.

 doi:10.20944/preprints202603.1720.v1

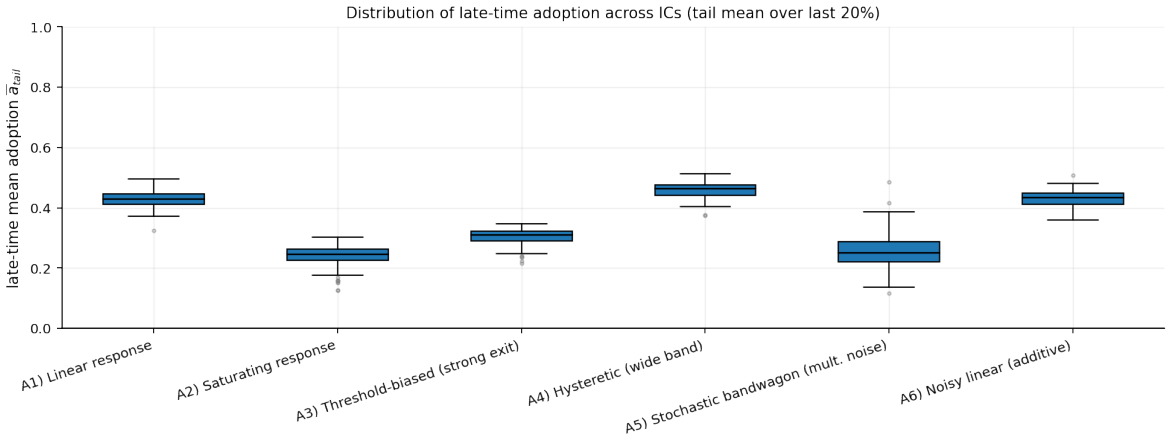

Figure A2. Late-time adoption across initial conditions: tail-mean participation under A1–A6. For each adoption law, the boxplot summarizes the distribution (over initial conditions) of the late-time mean adoption $\bar{a}_{\text{tail}}$, computed as the average of $a(t)$ over the final 20% of the horizon. This diagnostic complements regime and sliding statistics by quantifying which participation levels are associated with the observed anchoring and switching patterns.

Table A3. Anchoring dominance and late-time adoption outcomes (deterministic and hysteretic rules A1–A4). Reported are the mean share of time spent in attracting sliding on the valuation threshold Σ, together with late-time adoption statistics (mean and standard deviation over the final 20% of the horizon) computed across initial conditions. Exit frequencies from Σ are also reported.

Law	Mean slide share	Mean a_{late}	SD a_{late}	Exit to L	Exit to R
A1) Linear response	0.992	0.429	0.027	0.00	0.00
A2) Saturating response	0.985	0.237	0.036	0.00	0.00
A3) Threshold-biased (strong exit)	0.994	0.304	0.026	0.00	0.00
A4) Hysteretic (wide band)	0.991	0.460	0.028	0.00	0.00

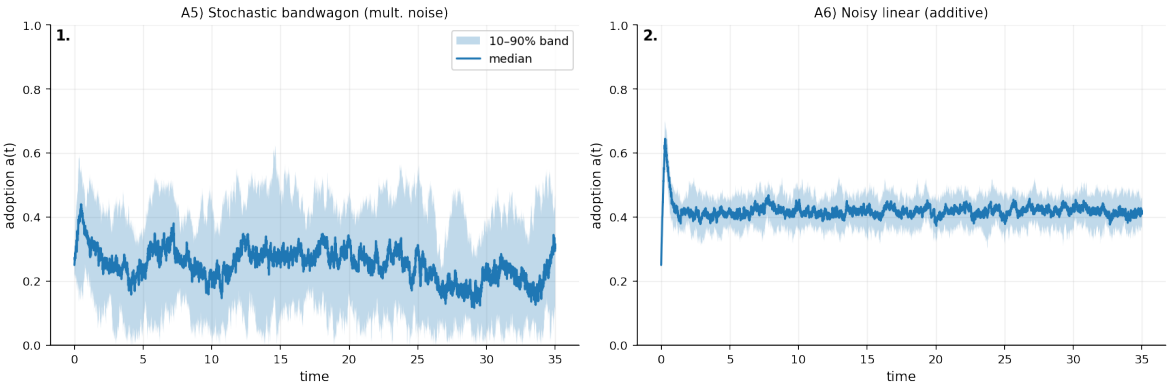

Figure A3. Monte-Carlo adoption envelopes under stochastic adoption (A5 and A6) from a common initial condition. For each stochastic adoption rule, the system is simulated from the same initial condition $(a_0, P_0) = (0.25, 0.55)$. Across Monte-Carlo replications, each run uses an independent noise realization and draws mild price-side heterogeneity in $(\beta_R, \bar{S})$. The shaded band reports pointwise 10–90% quantiles of $a(t)$ and the central curve reports the pointwise median. The envelopes isolate joint variability induced by adoption noise and market heterogeneity, highlighting differences in dispersion and drift between multiplicative (A5) and additive (A6) noise.

 doi:10.20944/preprints202603.1720.v1

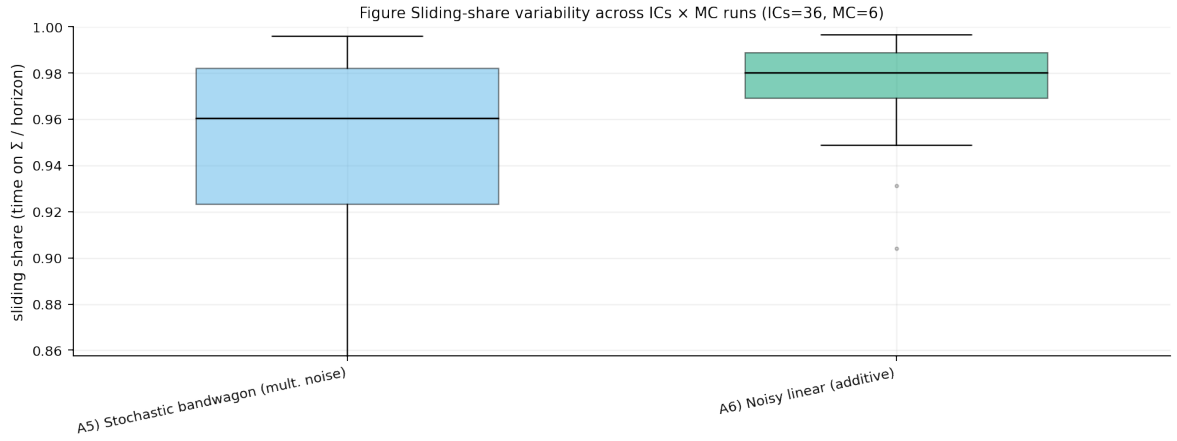

Figure A4. Distribution of sliding intensity pooled over initial conditions and Monte-Carlo runs (A5 vs A6). For each stochastic rule, the boxplot summarizes the distribution of the sliding-share statistic $T_{\Sigma}^{\text{slide}}/T$ pooled across all initial conditions and Monte-Carlo replications. Sliding is detected within a tight contact band and must satisfy the attracting inequalities $g_L(a, P_c) > 0$ and $g_R(a, P_c) < 0$, with a minimum episode duration to suppress spurious contact. Robust quantile-based axis limits are used to improve visibility of between-rule differences.

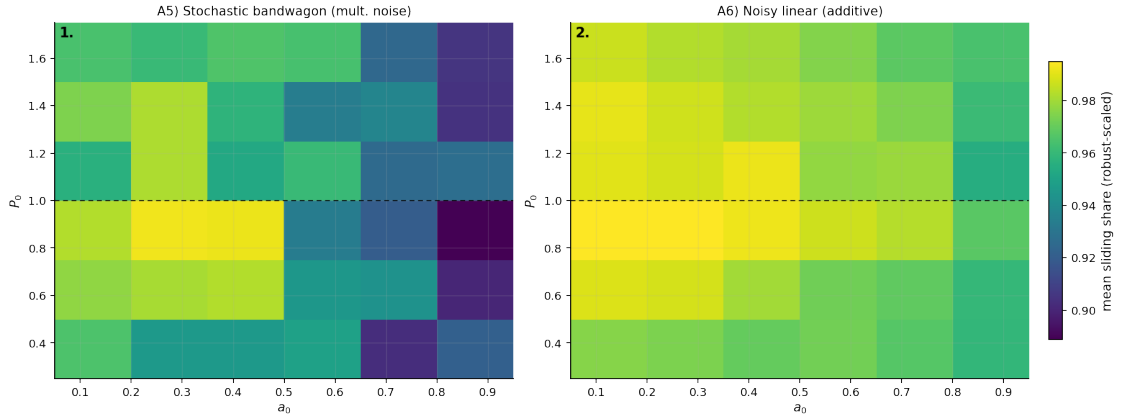

Figure A5. Initial-condition dependence of mean sliding intensity under stochastic adoption (A5 vs A6). Heat maps report the mean sliding share $\mathbb{E}[T_{\Sigma}^{\text{slide}}/T \mid (a_0, P_0)]$ computed by averaging across Monte-Carlo replications at each initial condition on the (a_0, P_0) grid. Colour limits use robust clipping to prevent a small number of extreme cells from saturating the scale. The dashed horizontal line marks the valuation threshold $P = P_c$.

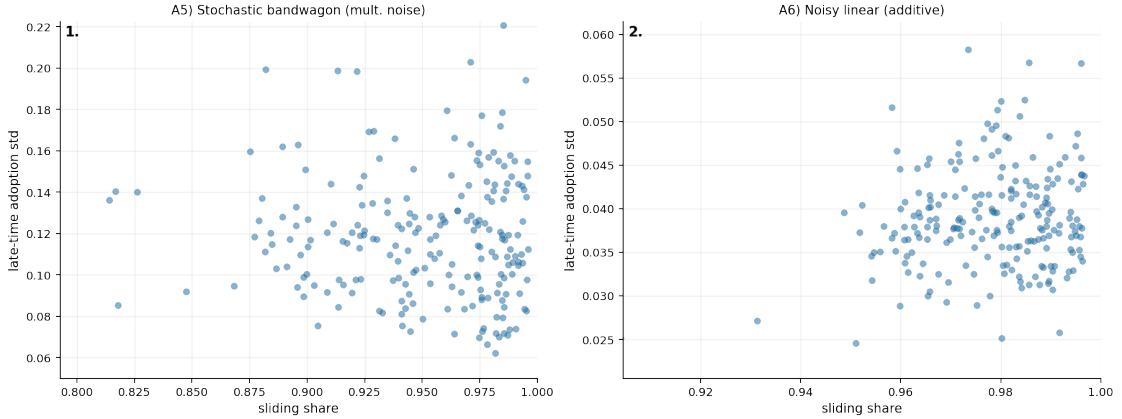

Figure A6. Trade-off between valuation anchoring and late-time participation volatility (stochastic rules). Each point corresponds to one simulation run (one initial condition and one Monte-Carlo replication). The x-axis reports sliding share $T_{\Sigma}^{\text{slide}}/T$ (valuation anchoring intensity), and the y-axis reports the standard deviation of adoption over the final 20% of the horizon (late-time participation volatility). Robust quantile-based axis limits reduce empty space while preserving the distributional pattern.

 doi:10.20944/preprints202603.1720.v1

Table A4. Stochastic anchoring intensity, volatility, and post-plateau exits (A5–A6). Reported are mean and standard deviation of the sliding share $T_{\Sigma}^{\text{slide}}/T$, late-time adoption statistics, late-time adoption volatility (standard deviation over the final 20%), and post-sliding exit behavior. Fractions are computed over the full ensemble of initial conditions and Monte-Carlo replications.

Law	Mean slide	SD slide	Mean a_{late}	SD a_{late}	Mean volatility	No slide	Exit L	Exit R
A5) Stochastic bandwagon (mult. noise)	0.948	0.044	0.255	0.084	0.119	0.00	0.00	0.54
A6) Noisy linear (additive)	0.978	0.013	0.426	0.042	0.039	0.00	0.00	0.04

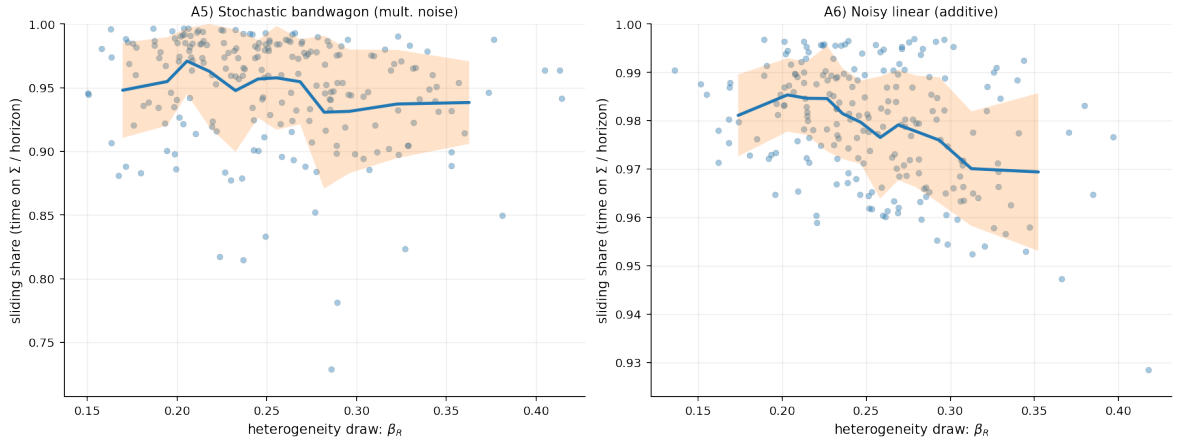

Figure A7. Sensitivity of valuation anchoring to heterogeneity in β_R (A5 and A6). Each point is one Monte-Carlo realization across initial conditions and heterogeneity draws, plotting sliding share $T_{\Sigma}^{\text{slide}}/T$ against the realized β_R. The solid curve reports equal-count binned means and the shaded band reports ± 1 standard deviation within bins. The vertical axis is restricted to $[0, 1]$ because sliding share is a proportion.

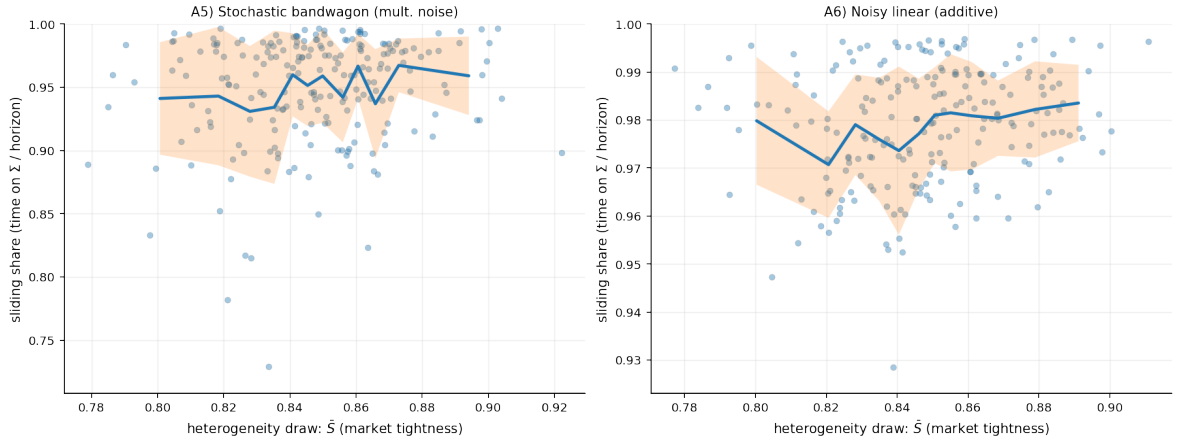

Figure A8. Sensitivity of valuation anchoring to market tightness heterogeneity $\bar{S}$ (A5 and A6). Points show Monte-Carlo realizations across initial conditions, plotting sliding share $T_{\Sigma}^{\text{slide}}/T$ against the realized draw of $\bar{S}$. The solid curve reports equal-count binned means and the shaded band reports ± 1 standard deviation within bins. The vertical axis is restricted to $[0, 1]$.

Table A5. Sensitivity of valuation anchoring to market heterogeneity (stochastic adoption rules). Reported are Pearson and Spearman correlations between sliding share $T_{\Sigma}^{\text{slide}}/T$ and heterogeneity draws in β_R and $\bar{S}$, computed across all initial conditions and Monte-Carlo replications for the stochastic adoption rules.

	slide_share vs. β_R		slide_share vs. $\bar{S}$	
Law	**Pearson**	**Spearman**	**Pearson**	**Spearman**
A5) Stochastic bandwagon (mult. noise)	−0.185	−0.234	+0.149	+0.118
A6) Noisy linear (additive)	−0.387	−0.338	+0.164	+0.175

 doi:10.20944/preprints202603.1720.v1

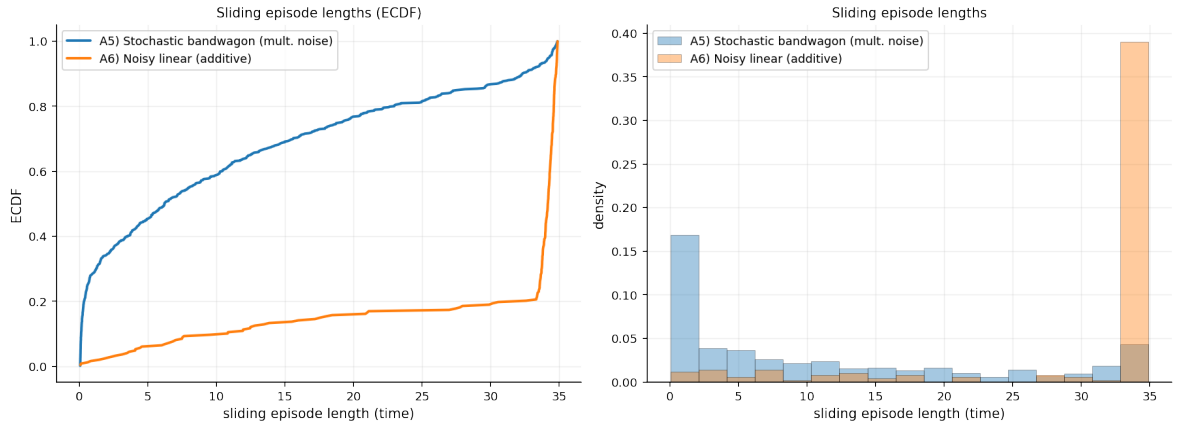

Figure A9. Sliding episode lengths under stochastic adoption (A5 vs A6): plateau persistence. A sliding episode is a maximal contiguous time interval during which the trajectory remains in attracting Filippov sliding on Σ. The left panel shows empirical cumulative distribution functions of episode lengths, and the right panel shows the corresponding normalized histograms. Differences between A5 and A6 quantify how the noise structure affects the persistence of valuation plateaus.

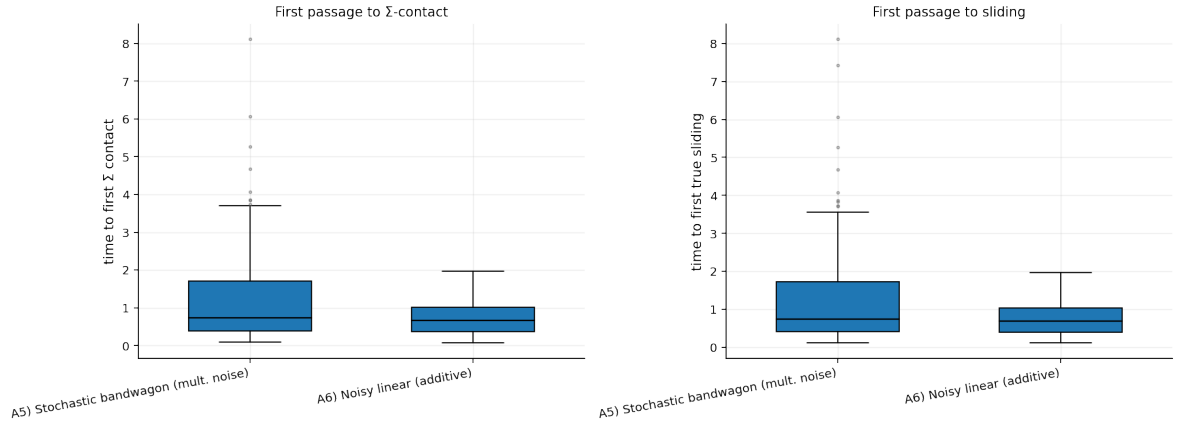

Figure A10. First-passage times to threshold contact and to genuine sliding. Boxplots compare (left) time to first contact with the switching manifold Σ and (right) time to first entry into an attracting Filippov sliding segment. The comparison highlights that geometric contact with Σ is not sufficient for valuation anchoring; anchoring requires the attracting inequalities defining sliding.

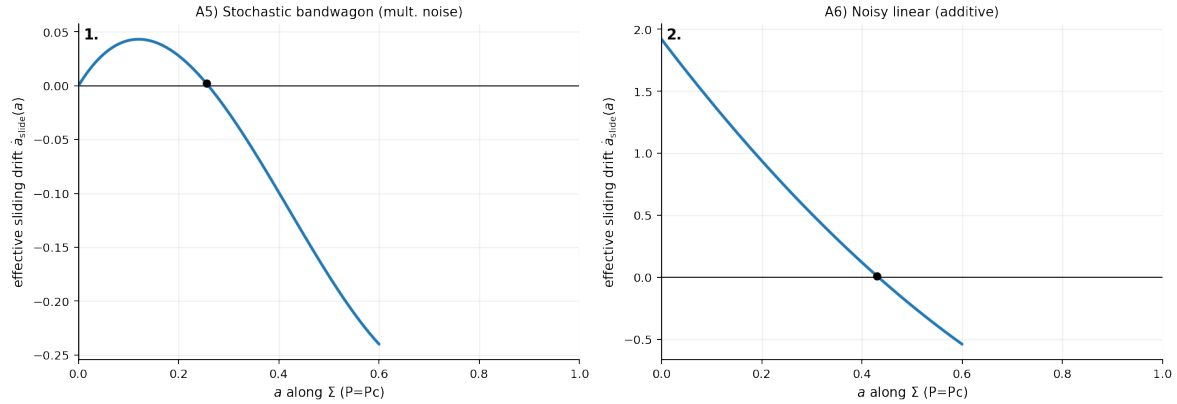

Figure A11. Induced sliding drift along the valuation threshold Σ. For each stochastic adoption rule, the Filippov sliding drift $\dot{a}_{\text{slide}}(a)$ induced on Σ is evaluated as a function of a and plotted only on the attracting sliding subset. Zeros of $\dot{a}_{\text{slide}}$ identify candidate sliding equilibria (pseudo-equilibria) that organize the long-run stochastic motion and the stationary adoption distributions reported below.

 doi:10.20944/preprints202603.1720.v1

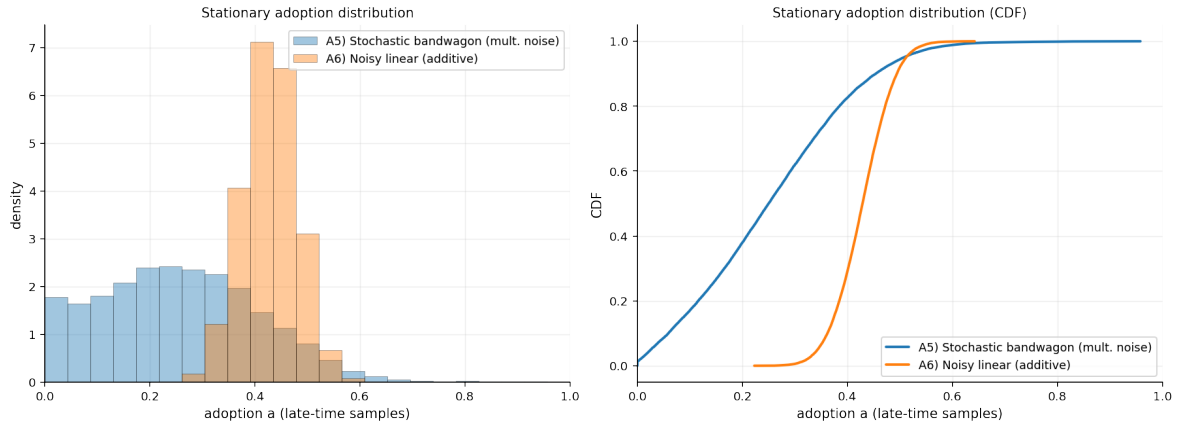

Figure A12. Stationary adoption distributions induced by stochastic sliding (A5 vs A6). Late-time samples of $a(t)$ are pooled across initial conditions and Monte-Carlo replications. The left panel reports normalized histograms and the right panel reports the corresponding cumulative distribution functions. These distributions summarize long-run participation outcomes generated by stochastic Filippov dynamics when valuation anchoring dominates.

Table A6. Threshold contact, sliding entry, and episode counts under stochastic adoption (A5 and A6). Reported are empirical probabilities of contacting Σ and entering attracting sliding, mean first-passage times to Σ and to sliding, and the mean number of distinct sliding episodes per trajectory, computed across all initial conditions and Monte-Carlo replications.

Adoption rule	p_{contact}	p_{sliding}	$\mathbb{E}[t_{\text{contact}}]$	$\mathbb{E}[t_{\text{sliding}}]$	$\mathbb{E}[N_{\text{episodes}}]$
A5) Stochastic bandwagon (mult. noise)	1.00	1.00	1.202	1.241	3.014
A6) Noisy linear (additive)	1.00	1.00	0.725	0.734	1.148

References

1. Aubin, J.-P., & Cellina, A. (1984). *Differential inclusions: Set-valued maps and viability theory*. Berlin, Germany: Springer-Verlag.
2. Barabási, A.-L., & Albert, R. (1999). Emergence of scaling in random networks. *Science, 286*(5439), 509–512. https://doi.org/10.1126/science.286.5439.509
3. Barberis, N., Shleifer, A., & Vishny, R. (1998). A model of investor sentiment. *Journal of financial economics*, 49(3), 307–343. https://doi.org/10.1016/S0304-405X(98)00027-0
4. Baumol, W. J. (1952). The transactions demand for cash: An inventory theoretic approach. *The Quarterly Journal of Economics, 66*(4), 545–556. https://doi.org/10.2307/1882104
5. Ben Youssef, A. (2022). Introducing Platforms: A transdisciplinary journal on platform management, services and policy and all related research. *Platforms, 1*(1), 1–4. https://doi.org/10.3390/platforms1010001
6. Biais, B., Bisière, C., Bouvard, M., Casamatta, C., & Menkveld, A. J. (2022). Equilibrium Bitcoin pricing. *Journal of Finance*. Available at SSRN: https://ssrn.com/abstract=3261063.
7. Brunnermeier, M. K., & Sannikov, Y. (2014). A macroeconomic model with a financial sector. *American Economic Review, 104*(2), 379–421. https://hdl.handle.net/10419/144448
8. Carlsson, H., & Van Damme, E. (1993). Global games and equilibrium selection. *Econometrica, 61*(5), 989–1018.
9. Cong, L. W., Li, Y., & Wang, N. (2020). Token-based platform finance. *NBER Working Paper No. 27810*. Cambridge, MA: National Bureau of Economic Research. https://doi.org/10.3386/w27810
10. Cong, L. W., Li, Y., & Wang, N. (2021). Tokenomics: Dynamic adoption and valuation. *The Review of Financial Studies, 34*(3), 1105–1155.
11. Cortés, J. (2008). Discontinuous dynamical systems. *IEEE Control Systems Magazine, 28*(3), 36–73. https://doi.org/10.1109/MCS.2008.919306
12. di Bernardo, M., Budd, C. J., Champneys, A. R., & Kowalczyk, P. (2008). *Piecewise-smooth dynamical systems: Theory and applications*. London, UK: Springer. https://doi.org/10.1007/978-1-84628-708-4
13. Erdős, P., & Rényi, A. (1959). On random graphs I. *Publicationes Mathematicae (Debrecen), 6*, 290–297.
14. Feenstra, R. C. (1986). Functional equivalence between liquidity costs and the utility of money. *Journal of Monetary Economics, 17*(2), 271–291. https://doi.org/10.1016/0304-3932(86)90009-9

 doi:10.20944/preprints202603.1720.v1

15. A. F. Filippov, "On certain questions in the theory of optimal control," *Journal of the Society for Industrial and Applied Mathematics, Series A: Control*, vol. 1, no. 1, pp. 76–84, 1963.
16. A. F. Filippov, *Differential Equations with Discontinuous Righthand Sides*, Kluwer Academic Publishers, 1988.
17. Goldstein, I. (2020). Initial coin offerings as a commitment to competition. Working paper, SSRN.
18. Han, Y., & Xie, L. (2025). Sustainable governance of digital platform ecosystem: A life cycle perspective through multiple governance parties. *Sustainability, 17*(8), 3628. https://doi.org/10.3390/su17083628
19. He, Z., & Krishnamurthy, A. (2011). A model of capital and crises. *Review of Economic Studies*, 79, 735–777.
20. He, Z., & Krishnamurthy, A. (2013). Intermediary asset pricing. *American Economic Review*, 103, 732–770.
21. Howell, S. T., Niessner, M., Yermack, D., & Wei, J. (2020). Initial coin offerings: Financing growth with cryptocurrency token sales. *The Review of Financial Studies, 33*(9), 3925–3974. https://doi.org/10.1093/rfs/hhz131
22. Krishnamurthy, A., & Vissing-Jorgensen, A. (2012). The aggregate demand for treasury debt. *Journal of Political Economy*, 120(2), 233–267.
23. Liu, Y., & Tsyvinski, A. (2021). Risks and returns of cryptocurrency. *Review of Financial Studies*, 34(6), 2689–2727. https://doi.org/10.1093/rfs/hhaa113
24. Makarov, I., & Schoar, A. (2020). Trading and arbitrage in cryptocurrency markets. *Journal of Financial Economics*, 135(2), 293–319. https://doi.org/10.1016/j.jfineco.2019.07.001
25. Morris, S., & Shin, H. S. (1998). Unique equilibrium in a model of self-fulfilling currency attacks. *American Economic Review*, 88(3), 587–597.
26. Nagel, S. (2016). The liquidity premium of near-money assets. *Quarterly Journal of Economics*, 131(4), 1927–1971.
27. Osler, C. L. (2003). Currency orders and exchange-rate dynamics: Explaining the success of technical analysis. *Journal of Finance*, 58(5), 1791–1820. https://doi.org/10.1111/1540-6261.00588
28. Pagnotta, E., & Buraschi, A. (2018). An equilibrium valuation of bitcoin and decentralized network assets. Working paper, SSRN. https://ssrn.com/abstract=3142022
29. Pagnotta, E. S. (2022). Decentralizing money: Bitcoin prices and blockchain security. *The Review of Financial Studies, 35*(2), 866–907.
30. Panori, A. (2024). Platforms enhancing proximity in the digital era. *Platforms*, 2(1), 1. https://doi.org/10.3390/platforms2010001
31. Parker, G. G., Van Alstyne, M. W., & Jiang, X. (2017). Platform ecosystems: How developers invert the firm. *MIS Quarterly*, 41(1), 255–266. https://doi.org/10.25300/MISQ/2017/41.1.13
32. Rochet, J.-C., & Tirole, J. (2003). Platform competition in two-sided markets. *Journal of the European Economic Association*, 1(4), 990–1029. https://doi.org/10.1162/154247603322493212
33. Rochet, J.-C., & Tirole, J. (2006). Two-sided markets: A progress report. *RAND Journal of Economics*, 37(3), 645–667. https://doi.org/10.1111/j.1756-2171.2006.tb00036.x
34. Saleh, F. (2021). Blockchain without waste: Proof-of-stake. *The Review of Financial Studies, 34*(3), 1156–1190. https://doi.org/10.1093/rfs/hhaa075
35. Schilling, L., & Uhlig, H. (2019). Some simple bitcoin economics. *Journal of Monetary Economics*, 106, 16–26.
36. Shams, A. (2019). What drives the covariation of cryptocurrency returns. Paper presented at the Association of Financial Economists and American Economic Association Beyond Bitcoin Paper Session Conference.
37. Sockin, M., & Xiong, W. (2020). A model of cryptocurrencies. *NBER Working Paper No. 26816*. National Bureau of Economic Research. http://www.nber.org/papers/w26816
38. Sontag, E. (2010). Contractive systems with inputs. In *Perspectives in Mathematical System Theory, Control, and Signal Processing* (pp. 217–228). Lecture Notes in Control and Information Sciences, 398. Springer-Verlag, Berlin.
39. Stiefenhofer, P., & Giesl, P. (2019). Economic periodic orbits: A theory of exponential asymptotic stability. *Nonlinear Analysis and Differential Equations*, 7(1), 9–16.
40. Stiefenhofer, P. (2020). Economic stability of non-smooth periodic orbits in the plane: Omega limit sets part I. *Nonlinear Analysis and Differential Equations, 8*(1), 41–52. Hikari Ltd. https://doi.org/10.12988/nade.2020.91121
41. Stiefenhofer, P. (2020). Economic stability of non-smooth periodic orbits in the plane: Omega limit sets Part II. *Nonlinear Analysis and Differential Equations*, 8(1), 53–65.
42. Stiefenhofer, P. (2025). Exponential stability of nonsmooth periodic orbits in the complex space. *Physics Letters A*, 130935.
43. Stiefenhofer, P. (2025). Spectral contraction framework for planar Filippov systems: Existence and stability of nonsmooth periodic orbits. *Communications in Advanced Mathematical Sciences*, **8**(4), 189–209.

 doi:10.20944/preprints202603.1720.v1

44. Sun, Y. (2025). A dynamic analysis of cross-category innovation in digital platform ecosystems. *Journal of Theoretical and Applied Electronic Commerce Research*, 20(3), 229. https://doi.org/10.3390/jtaer20030229
45. Tobin, J. (1956). The interest-elasticity of transactions demand for cash. *Review of Economics and Statistics*, 38, 241–247.
46. Walsh, C. E. (2003). *Monetary theory and policy* (2nd ed.). Cambridge, MA: MIT Press.
47. Watts, D. J., & Strogatz, S. H. (1998). Collective dynamics of 'small-world' networks. *Nature*, 393(6684), 440–442.
48. Zhou, Y., Wang, L., & Chen, M. (2025). Innovation in platform ecosystems: Roles of complementors and sustainability. *Sustainability*, 17(5), 2279. https://doi.org/10.3390/su17052279